Wischke, C.:
Concepts for efficient preparation of particulate polymer carrier systems by droplet-based microfluidics.
In: International Journal of Pharmaceutics. Vol. 584 (2020) 119401.
First published online by Elsevier: 05.05.2020

https://dx.doi.org/10.1016/j.ijpharm.2020.119401

Concepts for efficient preparation of particulate polymer carrier systems by droplet-based microfluidics

Christian Wischke [1]

[1] Institute of Biomaterial Science and Berlin-Brandenburg Centre for Regenerative Therapies, Helmholtz-Zentrum Geesthacht, Kantstr. 55, 14513 Teltow, Germany

E-mail: christian.wischke@hzg.de

Abstract.

Droplet-based microfluidics has grown out of its infancy as technical solutions became available for a broad community of researchers aiming at highly defined structures of polymer-based drug carrier systems. While the beauty of obtained particles and the precision of their (continuous) production may be very fascinating from a scientific perspective, microfluidics is further developing towards the use in production processes. This review summarizes recent concepts and developments in droplet-based microfluidics covering theoretical aspects of the operation principle as well as approaches to increased throughput and thus to enable efficient production. The application of microfluidic templating for preparing functional polymer particles including dispersions of preformed polymers, multicompartment particles and the use of template droplets as microreactors for carrier synthesis are also included. When operated at high-throughput, in a continuous process and with excellent control over particle properties, microfluidics may become a preparation technique for particulate carriers competitive to batch emulsification not only in research but also for commercial fabrication, e.g., of individualized, patient-specific formulations.

Keywords: droplet-based microfluidics, high-throughput, polymer particles, controlled drug release

1. Introduction

The preparation of particulate carrier systems by conventional batch emulsification of polymer/drug combinations has been the basis for injectable sustained release formulations, which are successfully used in the clinics for local and systemic treatment of diseases (Wischke and Schwendeman, 2008) (Ramazani et al., 2016) (Lee et al., 2016). As part of these batch production processes, the dispersion of polymer solutions into nascent particles is performed by application of high (non-uniform) shear stresses and/or by phase separation. As a consequence of non-uniform/statistic events, the sizes and morphologies of individual particles within a batch can substantially vary from each other, particularly when multicomponent carriers are to be prepared (Qi et al., 2019). In fact, particle sizes and drug distribution within polymeric carriers can strongly affect the drug release features (Park et al., 2019). This calls for technologies that would allow better homogeneity of particles within a produced batch, a reproducible tailoring of particle sizes, and the design of well-defined internal structures in case of multicomponent carrier matrices.

Microfluidic techniques opened up a multitude of opportunities to enhance and accelerate the research in pharmaceutical sciences, including drug discovery, drug synthesis and in vitro assays (Nys and Fillet, 2018). For drug formulation into particulate carrier systems, both phase separation/self-assembly processes and dispersion processes can be realized in microfluidic channels, which allow the embedding of drug molecules into polymeric matrices (Liu et al., 2017) (Damiati et al., 2018).

In this review, the focus will be on microfluidic dispersion of different phases into droplets. These droplets incorporating either polymerizable monomers, functionalized telechelics, or preformed polymers can subsequently be transferred by crosslinking and/or solvent removal into polymer particles of highly defined structure and size, typically in the micrometer range (Li et al., 2008a). Given the fact that some materials are challenging to disperse, customized devices and emulsification concepts may allow preparing particles also from such materials (Abate et al., 2011).

Aside from the experimental beauty and opportunities arising for research, the commercial applicability of droplet-based microfluidics for preparing polymeric carrier systems may depend on a number of additional aspects. This includes technical boundaries of the technology, including the question of throughput, as well as financial aspects regarding investments and production costs even for high-value products. In this respect, the rate of droplet formation remains key to productivity of microfluidic particle preparation. It is linked to process parameters, device design, and, importantly, the properties of the materials to be dispersed. Still, as literally monodisperse droplets of two-phase or multiple phase emulsions can be continuously templated in microfluidic channels (Datta et al., 2014) (Wang et al., 2011) and a toolbox of concepts to increase throughput has become available, droplet-based microfluidics can be expected to be increasingly used both in academic research and, as currently ongoing, in pharmaceutical development.

In this review as part of the Special Issue '*Europe'* of *International Journal of Pharmaceutics*, microfluidic concepts for preparing particulate carrier systems will be summarized, highlighting their significant development towards applications in the last 5 years. While a substantial set of work in the field of droplet-based microfluidics including many ground breaking findings originate from outside of Europe, a research community as well as industrial contributing players have established in Europe over the last one or two decades. At current, start-up incubators on microfluidics are growing. European companies have made various instrumentation commercially available for research and development, including microfluidic chips, pressure driven pumps, and even full-pack microfluidic production stations for polymer particles. By acknowledging the research conducted by an increasing number of European and international research groups, this review will concentrate on recent concepts and developments in droplet-based microfluidics covering some theoretical aspects of the operation principle, strategies to increased throughput, and the application of microfluidic templating for preparing particulate drug carriers.

2. Operation principle of common microfluidic droplet generators

In microfluidic droplet generators, droplets are produced one after the other. This principle is different from classical mixers, e.g., rotor-stator homogenizers, where numerous droplets are generated at the same time in different positions of the vessel. In droplet-based microfluidics, the dispersion of two or more immiscible phases is conducted in channels of well-defined geometries under continuous flow. This flow condition is characterized by balanced viscous forces, inertial forces, interfacial tensions and, in many cases, contributions by buoyancy. The flow conditions of two phase systems in microfluidic capillaries can be described by a number of dimensionless numbers such as the capillary number *Ca* and the Weber number *We*, as will be illustrated in later sections of this review. Those numbers can be determined from the interfacial tension σ between the two phases, the channel diameter d, the viscosity η, the velocity v, and the density ρ of the respective fluid.

$$Ca = \frac{\eta \cdot v}{\sigma} \qquad (1)$$

$$We = \frac{\rho \cdot v^2 \cdot d}{\sigma} \qquad (2)$$

The *Ca* represents the viscous shear forces in relation to surface tension. Ca is of interest for the outer fluid, also named continuous phase, as it acts on the phase that should be dispersed into droplets (inner fluid, dispersed phase). The *We* of the inner fluid represents the inertial forces in relation to surface tension. A more extensive description of physical parameters, dimensionless numbers and their contribution to droplet formation and droplet sizing in relation to capillary dimensions can be found in previous reviews (Zhu and Wang, 2017).

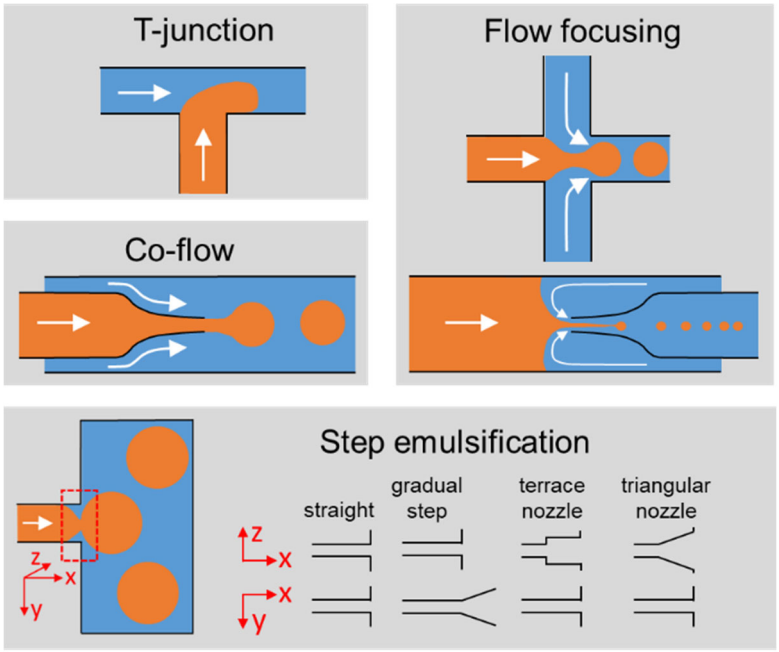

Fig. 1: Schemes of droplet formation at exemplary channel geometries. Blue: Continuous phase; Orange: Dispersed phase.

Depending on the channel geometry and operation mode, different droplet formation mechanisms/regimes are involved, of which a few will be briefly summarized here (Fig. 1). In microchannels with T-shaped junctions, the dispersed phase is typically fed perpendicularly into a straight channel that is well-wetted by the continuous phase. At high *v* and thus high *Ca*, droplet formation mainly bases on shear stress by the cross flow of the continuous phase. However, more commonly, T-junctions are employed in a slow and well controlled operation mode below a critical value of *Ca*, where the thread of the dispersed phase introduced at T-junctions results in a pressure drop along this channel section. Under these conditions, the droplet break-up is eventually dominated by a squeezing of the neck of the thread by the continuous phase (Garstecki et al., 2006).

Other widely employed channel geometries are axisymmetric co-flow as well as focused-flow geometries, which can be constructed, e.g., from glass capillaries (Shah et al., 2008) (Martino et al., 2014) (Benson et al., 2013). Additionally, cross junctions or ψ-shaped junctions with a flow focusing effect can be obtained, e.g., by soft lithography in polydimethylsiloxane (PDMS) (Tang and Whitesides, 2010). In focused flow devices, the thread of disperse phase is

enveloped by the continuous phase, which practically has the same flow direction at least at the site of dispersion, even if feeding channels for the continuous phase may be arranged in different angles for practical reasons. Depending on the employed flow rates, different operation principles can be distinguished: At slow flow, channel plugging and squeezing of the dispersed phase thread by the surrounding continuous phase can account for emulsification (Romero and Abate, 2012). When operated in the dripping regime, droplet break-up occurs by shear forces acting on the dispersed phase thread at the junction or orifice, where the immiscible phases meet. This dripping mode, which is characterized by low *Ca* and *We*, is most commonly used to produce practically monodisperse particles. They can be size-controlled within certain boundaries by flow rates and channel dimensions. At high flow rates in the jetting regime, a long thread of the disperse phase is formed and droplet formation occurs further downstream, which is typically less controlled as mainly driven by Rayleigh-Plateau instabilities. In any case, narrow orifices in focused-flow devices can assist in emulsification by increased shear and thread elongation. Furthermore, focused flow set-ups allow for droplet sizes smaller than the orifice diameter in both coaxial glass capillary assemblies (Shah et al., 2008) and PDMS devices (Tran et al., 2014).

In step emulsification, droplets can be formed at low frequencies without relevant contributions of shear forces by the continuous phase. Here, the disperse phase enters from a feeding channel through an opening of various possible geometries (e.g., straight channel (Mittal et al., 2014), terrace nozzle (Kobayashi et al., 2012), triangular nozzle (Amstad et al., 2016)) into a much wider channel, representing a step towards reduced spatial confinement. As droplet size can rapidly increase at the orifice, a jump in Laplace pressure of the liquid thread occurs, eventually causing its upstream necking and break-up through Rayleigh-Plateau instabilities (Dangla et al., 2013).

The concepts introduced above can be categorized as ‘passive’ droplet formation techniques, where physical principles such as interfacial tension result in fluid instability and drive the break-up of thin threads of solvents into droplets. It should be noted that in addition to those

concepts, also ‘active’ principles based on additional energy triggers (e.g. electric, magnetic, thermal) are explored for, e.g., on-demand droplet formation (Zhu and Wang, 2017).

3. Concepts to increase throughput

The capacity to obtain monodisperse droplets of predefined sizes is a main benefit of passively driven microfluidic emulsification. Most microfluidic devices can disperse fluids at rates that require high-speed cameras for detailed examination of the droplet formation. Still, as drops are formed one after the other, the overall throughput of a single channel does not compare with the quantities obtained in batch emulsification processes applied, e.g., for pharmaceutical sustained release carrier products (Takechi et al., 2002).

Changing one parameter directly linked to throughput in microfluidics, i.e., simply increasing the flow rates, may not necessarily result in higher output of the desired product. The size of droplets is determined by the device geometry in combination with process parameters (e.g. flow rates, flow rate ratios) and fluid properties (e.g. viscosities, interfacial tension). Enhancing the flow rate of one phase (i.e., altered flow rate ratio and/or capillary number) may be associated with an alteration in droplet size or transition in droplet formation modes (Utada et al., 2007) (Loizou et al., 2018). For instance, increasing capillary numbers of the continuous phase and the flow rate ratios caused a substantial reduction of droplet size in polycarbonate flow focusing devices as long as operated within the dripping regime. However, eventually jetting occurred and much larger, less homogeneous particles were obtained (Lashkaripour et al., 2019) (Fig. 2A). Increased back-pressure at high flow rates and, in consequence, bulging of some polymer materials like PDMS used to make channels by soft lithography may set additional limitations (Matthew et al., 2003). Furthermore, as it is true for most processes upon increasing speed, slight variation of experimental parameters like flow rate fluctuations or environmental vibrations can disturb a continuous operation (Li et al., 2014). Keeping this in mind, in a real life situation, faster production may be at the risk of an enhanced or unstable width of particle size distributions.

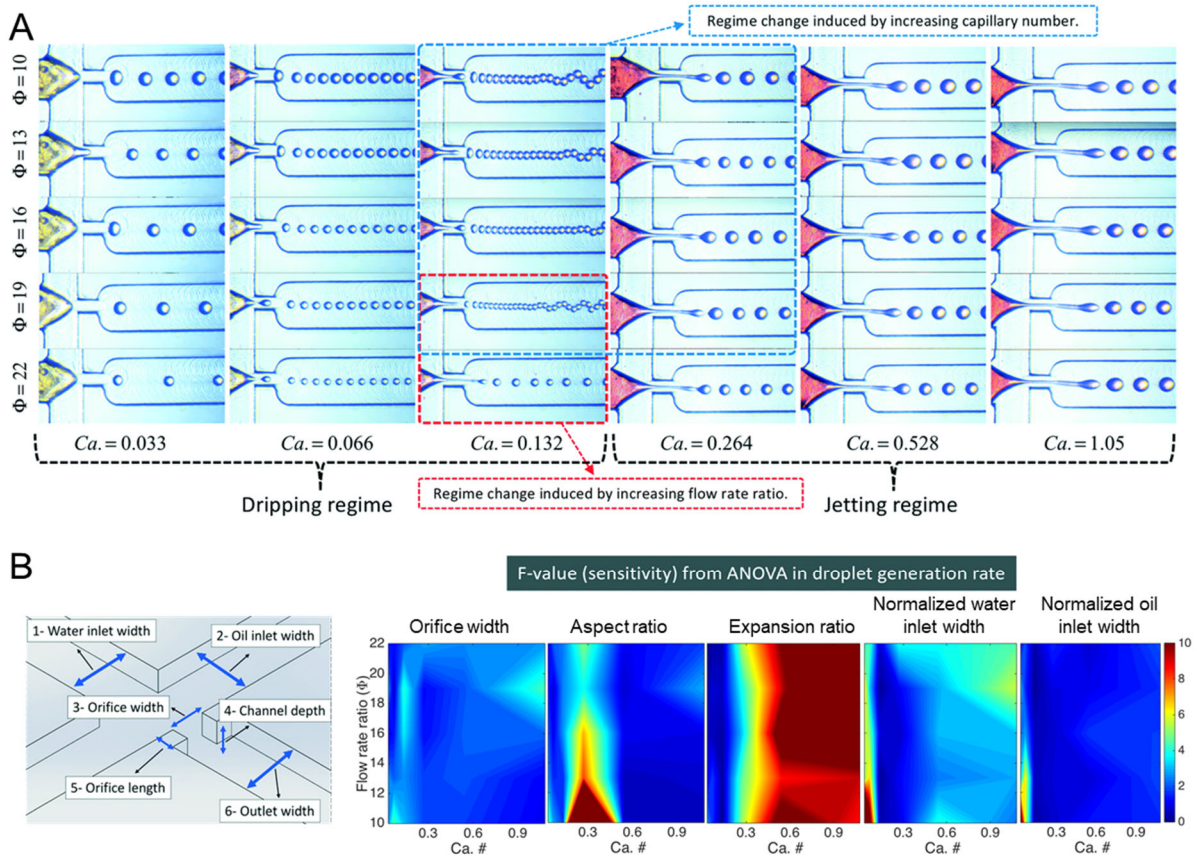

Fig. 2: Effect of increasing flow rates on droplet formation in a focused flow polycarbonate device. (A) Increasing flow rate of the continuous oil phase (increasing *Ca*) and flow rate ratio Φ of the water and oil phases result in altered particle sizes and regime changes from dripping to jetting conditions. (B) Identification of geometrical parameters affecting droplet generation rate to a high (red), medium (yellow and green) or limited (blue) extent at various flow conditions in the given device geometry: Orifice width (3); Aspect ratio of orifice width (3) and channel depth (4); Expansion ratio as the ratio of orifice width (3) and outlet channel width (6); Normalized widths of the water (1) and oil (2) inlets each determined in relation to the orifice width (3). Republished with permission of The Royal Society of Chemistry from (Lashkaripour et al., 2019); permission conveyed through Copyright Clearance Center, Inc.

Still, with most of the existing concepts to increase throughput as presented below, which focus either on enhancing the productivity per channel or on increasing the number of employed emulsification junctions (DFU, droplet-forming units), very homogeneous droplets can be obtained based on tailored design of droplet generator arrangements and well-balanced operation modes.

3.1. Per-channel productivity – balancing throughput versus precision

Altered junction geometries

Modifying the geometry of the microfluidic junctions such as the channel shape, height, width and cross-sectional area, respectively, are some of the main principles to affect the droplet formation. As illustrated in Figure 2B, geometrical parameters can either strongly or less extensively affect droplet generation rates, which allowed to cover a range of 10 – 800 formed droplets per second (Hz) in this specific flow focusing device (Lashkaripour et al., 2019).

In addition to channels with symmetric cross sections, single channels with triple- or multihelical cross-sectional designs were evaluated. In these channels, the primary axial flow has been overlaid with a secondary circumferential flow allowing for symmetry breaking and droplet formation from jets of immiscible fluids. The time of droplet formation decreased and thus the frequency increased systematically when the angle of the helix was increased (Ganneboyina and Ghatak, 2013).

Beside tailoring channel dimensions, alternative geometric arrangements may allow to increase throughput. One of those concepts deviates from using individual DFU with defined flow paths, but uses an array with several rows of pillars that break crude emulsion into fairly homogeneous droplets depending on pillar geometry (coefficient of variation $CV \geq 13\%$). This approach may be beneficial particularly for very viscous droplets, i.e., a ratio of viscosities of the dispersed and continuous phase $\eta_d/\eta_c >> 1$, which are often hard to emulsify with standard DFU. The applicability of such a device containing 40 rows of square pillars was exemplarily shown for methacrylate-based UV-crosslinkable monomers by preparing 20 µm polymer microparticles at high production rates of 15 $g \cdot h^{-1}$ (CV 20%) (Amstad et al., 2014).

A precise control of droplet size and size distributions can be obtained by a modification of the T-junction set-up, in which the straight main channel is connected with two side channels in a V-shape arrangement (Fig. 3). The main channel is supplied with continuous phase and one of the side channels located, e.g., in an angle of 60° to the main channel, provides the disperse phase. The second side channel acts as control channel and is supported with a valve and/or

pump suitable to inject or withdraw fluids. Depending on the operation mode of the control channel, at a fixed rate of continuous phase flow, the size of droplets can be tuned by droplet splitting at the V-junction. This setup allowed tuning particle sizes formed without major effect on generation frequencies of ~15 Hz. Additionally, also relatively higher frequencies of droplets formation for small particles were possible at V-junctions compared to a T-junction of similar dimensions (Ding et al., 2015). It should be noted that unsymmetrical droplet splitting, as used here, may be linked to a substantial quantity of dispersed phase being discarded, which could be critical in economic production.

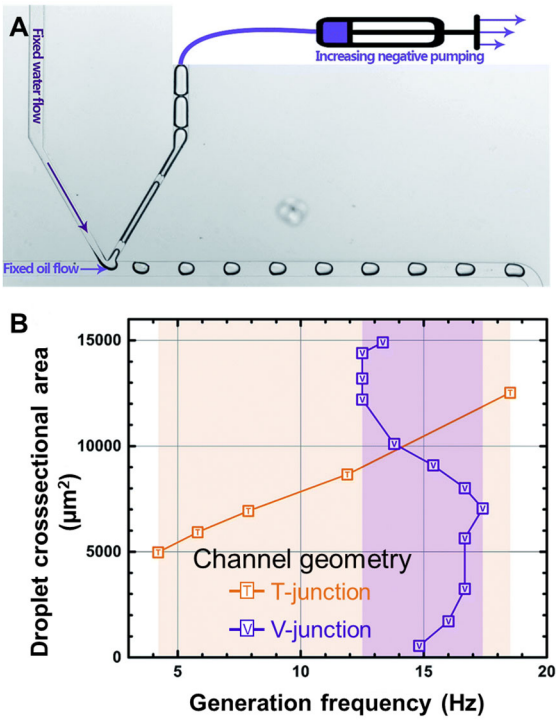

Fig. 3: V-channel geometry allowing manipulation of droplet size. (A) Image of V-channel set-up: A pump is connected to the control channel (upper right) applies suction ("negative pumping") for droplet splitting. By increasing suction rates, the size of droplets that are collected through the main channel are systematically reduced. (B) Dependency of droplet size and generation frequency for V-channel geometry compared to T-junction channels. Republished with permission of The Royal Society of Chemistry from (Ding et al., 2015); permission conveyed through Copyright Clearance Center, Inc.

Delayed surfactant addition

As indicated above, enhancing the flow rates to increase throughput will face limitations as a transition occurs from the well-controlled dripping regime towards the jetting regime with typically broader size distributions. The dripping-to-jetting transition was assigned to a state,

when either *Ca* of the outer fluid or *We* of the disperse phase or their sum is roughly in the range of 1 on a logarithmic scale (Utada et al., 2007). As has been shown in Equations 1 and 2, these numbers present the balance of viscous forces of the continuous phase (*Ca*) and the inertial force of the disperse phase (*We*), each normalized to the interfacial tension σ between the two phases. Based on this inverse relationship of *Ca* and *We* to σ, a high value of σ might in principle allow increasing the throughput (*v*) while keeping *Ca* and *We* low, i.e. remaining in the dripping regime. However, for kinetic stabilization of emulsion droplets and to avoid coalescence leading to broad droplet size distributions, typically a coverage of the interface of the immiscible phases with surfactants or steric stabilizers is needed, leading to reduced σ. By delayed surfactant addition in PDMS devices, a temporal and spatial separation of droplet formation at the nozzle and droplet stabilization by surfactants added further downstream can be obtained (Fig. 4). In this way, the per-channel rate of microgel precursor droplets could be increased roughly 8-fold, while preserving operation in the dripping regime (Seiffert et al., 2015). The concept has also been applicable to altered viscosity ratios of dispersed and continuous phases (Friess et al., 2016), suggesting a potential broad applicability to various types of materials. Via use of a shielding fluid, the concept can also be realized in focused flow glass capillary setups with two inner capillaries (Josephides and Sajjadi, 2015).

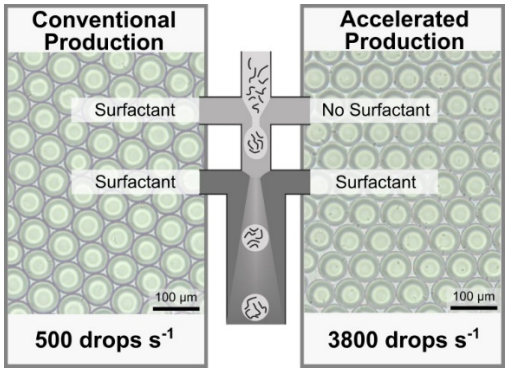

Fig. 4: Delayed surfactant addition to enhance per-channel productivity of a water-in-oil (w/o) emulsion as applied to prepare precursor particles subsequently gelled to poly(*N*-isopropylacrylamide) microgels. Left: Scheme of conventional production with surfactant added directly at the DFU. Right: Scheme of delayed surfactant addition, where surfactant containing continuous phase is added further downstream, thereby spatially separating droplet formation at enhanced rates and droplet stabilization. Reprinted from (Seiffert et al., 2015) with permission from Elsevier.

Droplet multiplication by droplet splitting

In a typical microfluidic setup, devices with larger cross-sectional areas of the emulsification nozzle allow for operation at relatively higher flow rates while remaining in the dripping regime. Under such conditions, the volume of the dispersed phase processed into particles is larger in a given time frame compared to small channels, but at the same time also the formed particles are larger. However, as mentioned above for V-shaped devices, preformed mother drops can be split into two or more daughter droplets, thus allowing for size reduction. Importantly, high precision of the splitting channel dimensions (cross-sectional area, length, angle) is required in order to provide a homogeneous splitting into daughter droplets of identical volumes. A number of split arrays purely based on passive splitting without additional energy sources have been evaluated, including series of Y or T-shaped geometries. The concept has been applied for single and double emulsions in planar arrays, where three or four subsequent binary splitting junctions resulted in the target droplet diameter of, e.g., 35 µm (Fig. 5A). Compared to production of the same particle size in a conventional channel, productivity by droplet splitting was 5 to 10 times higher, while acceptable CV in the range of 5-6% were obtained (Abate and Weitz, 2011).

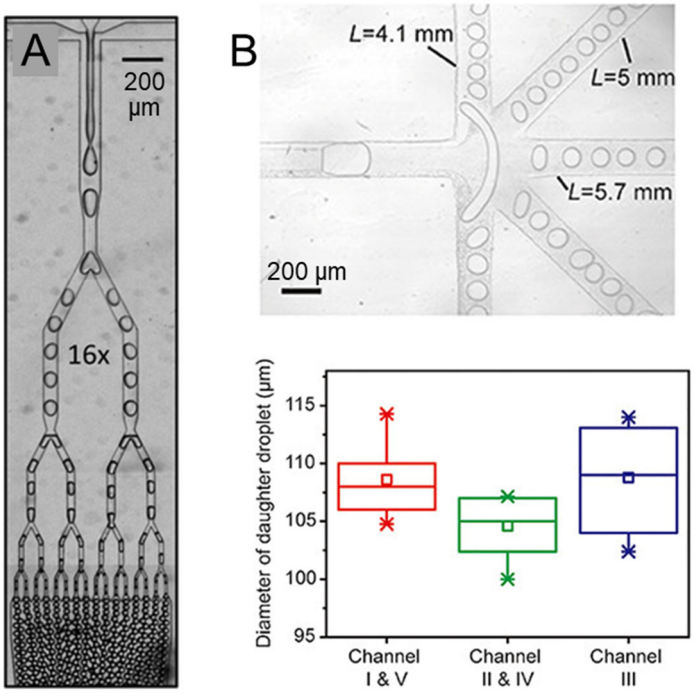

Fig. 5: Droplet splitting to increase numbers of produced particles. (A) Multiple binary splitting technique with each mother droplet split into 2^4 =16 daughter droplets. Republished with permission of The Royal Society of Chemistry from (Abate and Weitz, 2011); permission conveyed through Copyright Clearance Center, Inc. (B) Simultaneous mother droplet splitting in 5 daughter droplets, where hydraulic resistance of the respective outlet channels is balanced by outlet channel length to obtain similar daughter droplet sizes. Reprinted from (Li et al., 2019b), with the permission of AIP Publishing.

Single-step splitting not necessarily has to result in two daughter droplets only. In a multifurcating device with five outlet channels arranged in a planar semi-circle around the inlet channel, five similarly sized daughter droplets could be prepared from each mother droplet in a single step (Fig. 5B). Relatively large mother droplets of up to 350 µm in diameter had to be deformed extensively and temporarily plug all outlet channels to allow for a symmetrical break-up (Li et al., 2019b).

Flow obstacles, such as sharp tips or edges, provide further opportunities to divide droplets. For instance, a feeding glass capillary can be coaxially connected to a second downstream capillary containing, e.g., three star-shaped axisymmetric inner walls acting as knives. Here, relatively large single or double emulsion drops could each be split into three daughter droplets, with the three fractions having a narrow size distribution and almost identical mean diameters (Chen et al., 2016). In all those cases of droplet splitting, perfectly symmetrical arrangements and well controlled hydraulic resistance of the (several) outflow paths are an essential precondition to obtain comparable daughter particles. This may be some of the reasons why also active splitting principles based, e.g., on pneumatic valves, non-uniform temperature fields or acoustic waves are explored to tune daughter droplet sizes.

Controlled jetting and tip-streaming operation

Increasing the flow rates of the continuous and dispersed phase in a given channel geometry typically results in the formation of a thread of dispersed phase that expands into the collection channel. In this so-called jetting regime, the liquid jet experiences axisymmetric surface perturbations eventually leading to droplet break-up. The wavelength of these oscillations

correlates with the flow rate of the dispersed phase and is a parameter to predict droplet sizes formed in the jetting regime (Cordero et al., 2011) (Zhu and Wang, 2017).

In narrowing jets, where *Ca* of the continuous phase is large, viscous drag results in stretching of the liquid thread of the dispersed phase. In this operation mode, smaller particles can be obtained compared to the dripping regime. The concept is applicable also to double emulsions, where the transition from dripping to narrowing jets has been numerically described based on the *Ca* of the different phases and the device geometry (Nabavi et al., 2017a). Attention may need to be payed to small satellite droplets occasionally formed in narrowing jets in between the main drops.

In tip-streaming, the dispersed phase liquid is forming a sharp cone rather than a long thread. Out of the apex of this cone, a very fine jet expands and eventually breaks up into very small droplets. In order to achieve this mode, a compression of the liquid thread from all sites was found to be necessary, as realized in glass capillary microfluidics, specifically designed polymer-based channels, or hybrid devices (Xu et al., 2017b). By this method, hydrogel particles as small as ~180 nanometer (CV 2.8%) were obtained from very diluted solutions of poly(ethylene glycol) diacrylate (PEG-DA), when the pumping pressure ratio of dispersed and continuous phase was systematically decreased and devices with a low hydraulic resistance of the outlet channel were used (Jeong et al., 2012). However, narrowing jets and tip streaming typically operate stable only within a relatively narrow process window, and may be occasionally interrupted resulting in contaminations with large particles. An optical imaging of the cone interface in tip streaming in combination with an automated adjustment of dispersed phase pumping has been explored to tackle these issues (Moyle et al., 2013).

Both, narrowing jets and tip streaming mode allow increased frequencies of droplet production and higher throughput of the dispersed phase, while also enabling to prepare smaller sized particles that are not routinely assessable in the dripping regime. Broader size distributions than in the dripping regime may occur, e.g., CVs of 10-25% were reported for PEG-DA templated by narrowing jets and tip streaming (Wu et al., 2018). However, others reported

excellent polydispersity indices (PDI) < 0.04 for 200 nm droplets of a perfluorocarbon liquid prepared as contrast agent via tip streaming (Xu et al., 2017b). Thus, in optimized conditions and with ideally suited fluid properties, a particle uniformity may be reached by narrowing jets or tip streaming that is well acceptable particularly when compared to batch emulsification processes in pharmaceutical production.

3.2. Numbering-up – parallel operation based on complex device designs

The typical industrial scale-up concepts such as increasing vessel sizes cannot be applied in microfluidics, as channel dimensions sensitively affect droplet dimensions. Instead, scale-up can be achieved by numbering-up, i.e., a parallel operation of several individual emulsification junctions.

Since the supporting infrastructure such as pumps, pressure controller etc. are the most spacious and costly parts of the necessary equipment, one would prefer a parallel operation of several channels in a single device fed by one set of pumps over the use of multiple totally independent set-ups. In flow rate controlled dispersion, this is, however, associated with the challenge to ensure an identical hydraulic resistance at each dispersing site of the device in order to allow for identical droplet sizes. Therefore, a complex design and a precise construction of devices are needed.

One should be aware that an accidental partial or full blockage of single channels in a set of parallel channels connected by, e.g., a tree-like feeding system (Li et al., 2008b) can dramatically change droplet sizes obtained in the (partially) blocked and all other channels due to a shift of local flow rates, thus broadening the size distribution. This may lead to out-of-specification results for the entire production run. Additionally, it should be noted that pressure oscillations associated with droplet formations e.g., at T-junctions, if not perfectly synchronized at the different DFU, can effect particle size homogeneity in some parallelized devices (Barbier et al., 2006). An efficient filtering system for the provided fluids and a continuous monitoring of

obtained droplet sizes is mandatory to avoid or, at least, rapidly detect particle size inhomogeneities.

Parallelized glass capillary devices

A practical, lab-scale approach for parallelized devices, which is also suitable for operation with polymers dissolved in organic solvents, may be hand-build from glass capillaries arranged together on a microscope slide and all connected to the same inlet and outlet ports (Kim et al., 2013b). However, slight differences in orifices sizes, distances between the orifices in double emulsion set-ups, and unequal flow rates depending on the respective channel position relative to the device inlet are almost unavoidable for such systems and may contribute to a broadened size distribution of the formed droplets.

Spatial arrangement of feeding channels and DFU in flow rate dependent particle templating

Using soft lithography, many identical DFU can be realized in a single device typically replicated in PDMS. High precision device fabrication is needed as alterations of the nominal channel width/depth in the range of ± 2% can very strongly alter the flow rates, as shown by simulation for tree-like feeding channels. This phenomenon was much less pronounced for comb-like feeding channels, which connect with the DFU and the subsequent collection channels to a ladder-like network (Tetradis-Meris et al., 2009). However, in a ladder-like network, different channel lengths will always be present from the device inlet/outlet to each individual DFU. Accordingly, based on increasing hydraulic resistance with increasing distance from the device inlet, variation of local flow rates will increase with the number of parallel DFU in ladder-like networks. Some design strategies to tackle this issue are:

(1) Ladder-like channel networks employing large feeding/collection channels with low hydraulic resistance R_c per segment compared to the much higher hydraulic resistance R_u of the DFU. Accordingly, mainly the DFU and not the support channels account for local hydraulic resistance at different emulsification junctions. A ratio $R_c/R_u < 0.01 / 2 \cdot N$ was suggested for

preparing single emulsions in a DFU with a given R_u, in this case with fluid supply from a second layer of distribution channels (Fig 6A). This means that R_c has to be decreased proportionally (by larger width/height) when increasing the number N of parallel operated DFU to realize a final difference of R <1% between any DFU (Romanowsky et al., 2012). The feeding channels can also be placed in the same plane as the DFU, a design that allows coupling several units as desired (Femmer et al., 2015).

Ladder-like support structures have further been used to supply thousands of DFU created by deep reactive-ion etching (DRIE) at a very high DFU packing on silicon wafers (20,160 DFU on 6.3 x 5 cm^2) (Fig 6B). Here, again, a two layer design has been adapted, in which the DFU are connected to the supply channel with small connections (vias). The channels contain flow resistors with a rectangular cross-section and small width (e.g. 8 µm) upstream of the DFU. As hydraulic resistance in those rectangular channels primarily scales with channel width and throughput with channel height, both parameters can be (partially) decoupled. These devices allowed to prepare ~ 20 µm oil droplets (CV < 5%; dispersed phase throughput 1-5 l/h) in the dripping regime under pressure (Fig 6B), and were applicable to produce 5-9 µm poly(*ε*-caprolactone) (PCL) microparticles thanks to device stability in organic solvents (Yadavali et al., 2018) (Yadavali et al., 2019).

(2) Circular arrangement of the DFU on a microfluidic chip to have identical lengths of on-chip feeding channels and a common, large outlet port (Fig. 6C). Such devices are supported by a chip interface with concentric annular supply channels of minimized length and, again, show a sufficiently low R_c to allow local differences in R < 1% for the respective N of DFU (Nisisako et al., 2012). It should be noted that for the depicted single emulsion devices (Fig. 6C), the emulsification principle corresponds to that of a T-junction, but involves feeding of the disperse phase from two sides into the continuous phase operated in cross flow. The chips and holders can be made from glass and steel, respectively, which also supports the handling of various solvents not compatible with, e.g., PDMS based microfluidic chips. With such circularly arranged devices containing, e.g., 144 parallel channels, the production of ~90 µm acrylate-

based particles with a CV of 2.2% was demonstrated at a throughput of 180 ml/h (Nisisako et al., 2012) (Nisisako and Torii, 2008).

(3) Shared on-chip feeding reservoirs with integrated pillars and funnel-like ports towards the individual DFU (Fig 6D). Here, the pillars should realize a homogeneous flow distribution upstream of all channels. The pillars may also allow for filtering and removal of particles that may occasionally be present in the different phases as impurities, thus enhancing the robustness of the production process. In principle, two of such feeding structures could be arranged in a single plane, allowing for preparation of single emulsions. In a specific example, a chip with one feeding structure for the continuous phase was combined with a pressure chamber, in which the dispersed phase was delivered through drill-holes contacting the channel plane. This set-up with 10 parallel channels allowed for the production of ~50 µm droplets with a CV of 1.5% at a throughput of dispersed phase of 26 ml/h (Lim et al., 2015). With this technology, on-demand drop formation with either identical or different dispersed phases (e.g. for drug combinations encapsulated separately) at the different ports of the parallel device might be achieved.

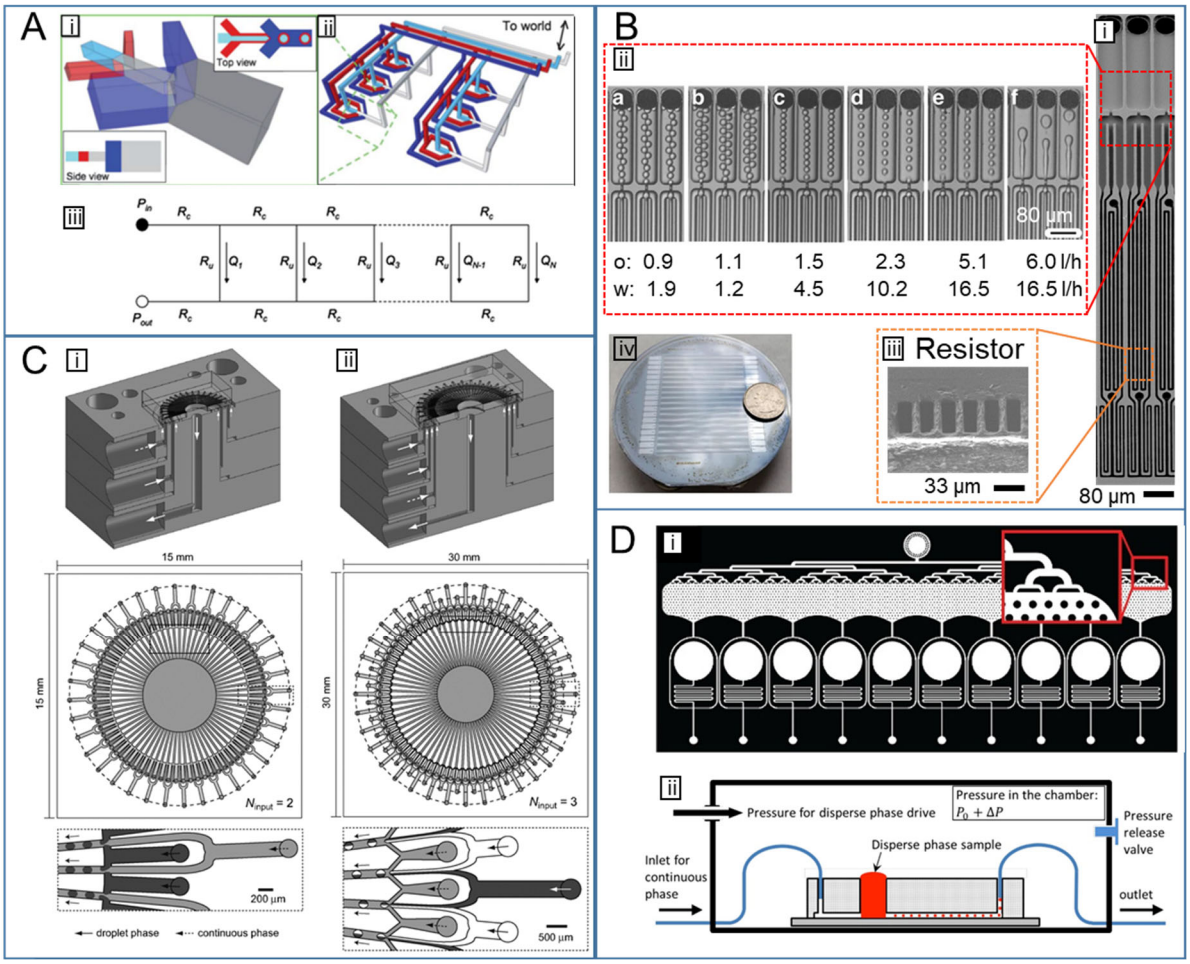

Fig. 6: Feeding channels and spatial arrangements for optimized parallel operation. (A) PDMS-device containing (i) double-emulsion DFU with (ii) ladder-like microchannel network for parallel operation. (iii) Model of hydraulic resistance R_c of supply/collection channel segments and R_u of the DFU; flow rate Q, N number of channels; $P_{in/out}$ are feeding and collection ports of the PDMS device. Republished with permission of The Royal Society of Chemistry from (Romanowsky et al., 2012) ; permission conveyed through Copyright Clearance Center, Inc. (B) Silicon-based rectangular array with 36x560 individual DFU supported by a ladder-like support structure. (i) Images of 3 DFU, each being 80 µm x 1.6 mm. (ii) Magnification of nozzles when operated for hexadecane (o-phase) emulsification in aqueous Tween 80 (w-phase) at the stated flow rates. (iii) Magnification of flow resistor channels upstream of each nozzle. (iv) Photograph of silicon chip. Adapted from (Yadavali et al., 2019) under a Creative Commons Attribution 4.0 International License (https://creativecommons.org/licenses/by/4.0/). (C) Glass/steel device with circular arrangement of DFU for parallel operation. (i) Single emulsion device. (ii) Device for 3 phases, here with microchip to prepare Janus particles. Republished with permission of The Royal Society of Chemistry from (Nisisako et al., 2012); permission conveyed through Copyright Clearance Center, Inc. (D) Device with (i) modified tree-like feeding structure with shared buffer reservoir containing pillars for fluid distribution and (ii) pneumatic feeding principle for the dispersed phase. Reprinted from (Lim et al., 2015), with the permission of AIP Publishing.

Parallelization of step emulsification

In contrast to flow focusing geometries, where the balance of flow rates and other parameters affect the droplet size in a sensitive manner, step emulsification is an alternative principle with a number of benefits. No shear forces of the continuous phase are needed, thus reducing the number of critical experimental parameters. However, the dispersed phase flow rate at a single DFU needs to be slow in step emulsification in order to allow for faster nozzle clearance than refilling. Still, minor flow rate alterations of the disperse phase have no strong impact on particle size at least when remaining in the dripping regime at low *Ca* (Kobayashi et al., 2012) (Amstad et al., 2016). Droplet diameters are dominated by device dimensions and, for a given fluid, were discussed to directly scale with channel height h either by the factor $h^{1/3}$ (terrace nozzle) or h^2 (triangle nozzle; see Fig. 1) due to the involved planes of drop confinement at the different nozzle geometries (Nakajima, 2017) (Amstad and Weitz, 2017). Based on the relative independence of droplet size and dispersed phase flow rate, undesired coupling of droplet pinch-off between different DFU can be avoided. Via surface modification of the device nozzles, the droplet sizes can be tuned since increasing contact angles between dispersed phase and substrate (i.e. nozzle dewetting by dispersed phase in favor of wetting by continuous phase) allows to produce smaller particles (Eggersdorfer et al., 2018). Combining triangular nozzles with a gradual step (larger height of nozzle opening) resulted in larger droplets at reduced frequencies (Eberhardt et al., 2019).

Considering those aspects, the power of step-emulsification is not necessarily found in its throughput per DFU but the scalability by parallelization of DFU without major issues of hydraulic resistance homogeneities for dispersed phase feeding. Accordingly, various types of parallel arrangements of nozzles have been reported. For instance, a PDMS device with a total of 550 triangular nozzles placed in two rows along a dead-end central feeding channel (“millipede device”) produced water-in-oil droplets of the desired diameter in the range of 20-150 µm, e.g., 150 µm droplets of PEG solution with a CV of 3% at a throughput of 150 ml/h. The authors speculate that, based on the dense packing of the DFU, further upscaling of this arrangement could lead to 600 liter per square meter and production hour (l/m^{2}h), while placing

the DFU like a membrane in between a feeding and a collection layer could lead to 11,000 l/m^2·h (Amstad et al., 2016) (Fig. 7A). Such a “membrane-like” vertical straight-through arrangement was realized with 24,772 terrace style nozzles in a 4x4 cm^2 silicon array (nozzle area 4 times 11x11 mm^2) integrated in a steel housing, which produced 1.4 l/h of a higher viscosity oily phase into oil-in-water emulsions (87 µm droplets, CV 2%), equaling 2,800 l/m^2·h (Kobayashi et al., 2012). The droplet diameter can be reduced to, e.g., 4-7 µm with finer nozzles, which needed to be numbered up to 176,176 DFU on a 11x11 mm^2 area to allow for an oil phase throughput of 1.5 ml/h in laboratory scale (Fig 7B) (Khalid et al., 2017). Terrace nozzles are also used in devices with dead-end supply channels and shared terraces for several DFU, demonstrating suitability for continuous preparation of ~5 µm particles from PCL and poly(*D,L*-lactide) (PLA) with stable sizes (CV ~2%) as investigated over several hours (Vladisavljevic et al., 2018).

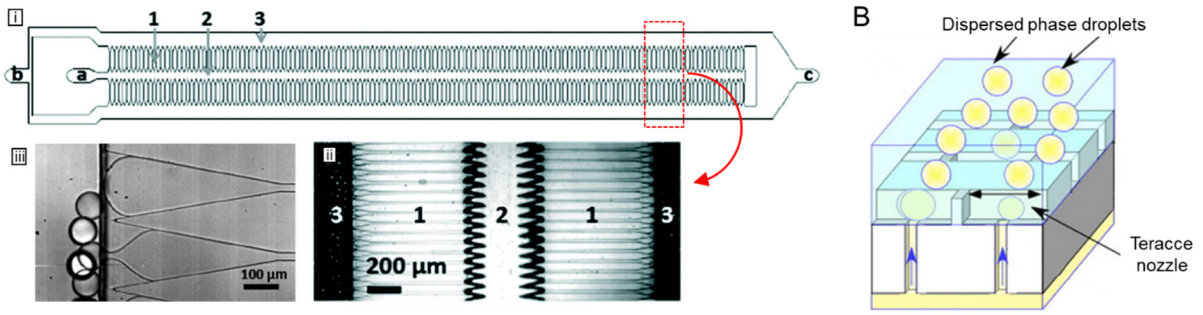

Fig. 7: Parallelization in step flow emulsification. (A) “Millipede” device (i) with two rows of DFU (ii) and triangular nozzles (iii). In-figure labels: a/b/c = inlet dispersed phase/inlet continuous phase/outlet; 1/2/3 = individual DFU/distribution channel for dispersed phase/collection channel with continuous phase. Republished with permission of The Royal Society of Chemistry from (Amstad et al., 2016) ; permission conveyed through Copyright Clearance Center, Inc. (B) Device with terrace shaped nozzles. Adapted with permission from (Khalid et al., 2017) © 2017 WILEY - VCH Verlag GmbH & Co. KGaA, Weinheim.

A number of practical issues may need to be considered in parallelized step emulsification. As no flow of the continuous phase is needed to shear-off nascent droplets, high volume fraction emulsions can be achieved. Still, droplet transportation away from the DFU is required. This droplet clearance has been realized by a pressure-expandable vessel for droplet collection resulting in a net slope at the DFU (Dangla et al., 2013). More commonly, a flow of medium

through the collection area is applied. In fact, if the formed droplets are not removed from the collection area at sufficient rates, they may approximate in the channel. This sets high demands for efficient droplet stabilization such as by surfactants, may disturb the formation of subsequent droplets by collision events (Mittal et al., 2014), or could even clog the channel in case of rapidly solidifying formulations. In some studies, the flow rate of the continuous phase was found to be optimal at 1.5x to 10x of the dispersed phase (Eberhardt et al., 2019). The aforementioned vertical straight-through operation (Kobayashi et al., 2012), particularly for dispersed phases with significant buoyancy, can help to prevent such effects as also shown in a recent version of the millipede device (Stolovicki et al., 2018).

Device stability to solvents is another relevant point for the fabrication of particles from hydrophobic polymers, as frequently used in controlled drug delivery. High solvent resistance, at least for common fluids in pharmaceutical drug particle preparation, can be found in silicon devices (Kobayashi et al., 2012), which may also be sterilized based on their heat stability. Also, metal-based terrace devices made from stainless steel (Li et al., 2019a) or, probably with lower stability, from aluminum (Zhang et al., 2019) are of potential relevance in this respect. The millipede device, if fabricated from glass, can also be operated with organic solutions as shown by their use for PCL microparticle preparation (Ofner et al., 2017).

The viscosity of the dispersed phases, which may be high in particle production from concentrated polymer solutions, can heavily influence the possible flow rates and thus the throughput of step emulsification devices in the dripping regime. For instance, in a direct comparison of dichloromethane (0.56 mPa/s), *n*-decane (0.92 mPa/s) and paraffin oil (~50 mPa/s) in DFU with triangular nozzles, increasing flow rates in the 1-12.5 µl/min per DFU resulted in identically increasing droplet sizes for the different solvents at a given condition, with the exception that paraffin oil could only be processed in a controlled manner up to 2 µl/min (Eberhardt et al., 2019). When comparing *n*-tetradecane (2.7 mPa/s), medium chain triglyceride (MCT, 20 mPa/s) and soybean oil (50 mPa/s) in terrace nozzles, the possible flow rates for particle preparation dropped to 33% (MCT) and 6% (soybean oil) relative to *n*-tetradecane, which was in accordance with predictions by computational fluid dynamics

(Vladisavljevic et al., 2011). At the same time, when the geometries and flow resistances of parallelized step emulsification devices were optimized for oils, not all channels may be productive during operation with low viscosity liquids when applying a slow flow rate regime (Vladisavljevic et al., 2011). This indicates boundaries of the versatile use of a given step-emulsification device.

A number of geometrical alterations of triangular nozzle devices were suggested in order to produce droplets from high viscosity liquids. Considering the relevance of good wetting of the nozzle by the continuous phase, concepts were derived in which the continuous phase is added earlier in the step-emulsification channel to surround the dispersed phase liquid at the step (Li et al., 2015) or in which bypass channels are used to feed the continuous phase into the nozzle opening for better wetting of nozzle walls and centering of nascent droplets (Dutka et al., 2016). Such backflow channels have also been successful in parallelized triangular nozzles to process high viscosity liquids (155 mPa/s) (Hati et al., 2018).

In order to allow for more complex particle structures being prepared or to enable the entrapment, e.g., of hydrophilic components in hydrophobic matrix materials, double emulsions are a suitable technique. Given the need of preferential wetting of the nozzle by the respective continuous phase at each emulsification step (w/o; [w/o]/w), integrating a cascade of oppositely wettable micro-sized nozzles in highly parallelized one-piece step-emulsification devices is challenging, which promotes the use of modular systems. Accordingly, direct coupling of two step-emulsifiers either based on PDMS or on glass have been used to prepare w/o/w and o/w/o emulsions, respectively, in some cases tailored to contain either one or multiple inner phase droplets (Eggersdorfer et al., 2017) (Ofner et al., 2019).

4. Application of droplet-based microfluidics for preparing functional polymer carriers

Microfluidics are extensively explored in life sciences for various applications, including the microfluidic encapsulation of active compounds into microparticles, the embedding of living cells in hydrogel carriers (Hasturk and Kaplan, 2019) (Alkayyali et al., 2019), or the microfluidic

preparation of nanoparticulate drug carriers through nanoprecipitation by non-solvents or colloidal assembly (Liu et al., 2018) (Li and Jiang, 2018). When using gas as continuous phase, amorphous drug nanoparticles can be obtained by microfluidic spray drying for otherwise crystalline compounds (Amstad et al., 2015) (Steinacher et al., 2019), which is of interest to accelerate the dissolution of hydrophobic drugs. Furthermore, when a jet of fluid is impacted by droplets ejected from a laterally placed vibrating nozzle, core-shell or multicompartment particles could be prepared in a gas-phase without the need of microchannels or immiscible continuous phase solvents (Visser et al., 2018) (Kamperman et al., 2018). Given the substantially growing number of microfluidic concepts to prepare functional polymer-based carrier particles, here, a focus will be placed on selected examples of droplet-based particle preparation approaches that could contribute to either improve existing or to realize new features of drug carrier systems. For cell encapsulation, nanoprecipitation, and in-air microfluidics, readers may be referred to the literature cited above.

When polymer solutions are processed in droplet-based microfluidics, the submicron size-range can be reached by using highly diluted polymer solutions as dispersed phases. This principle is based on massive droplet shrinkage upon solvent extraction, which is quite inefficient, e.g., in terms of mass throughput. Therefore, the focus of the following sections will be on microparticles, where the ability of microfluidics of precisely constructing single or multiple phase droplets can be fully utilized. Accordingly, a broad design space of microparticle shapes and ultrastructures may become accessible (Fig. 8) (Li et al., 2018), which should allow tailoring physicochemical properties of such carriers and the drug release function.

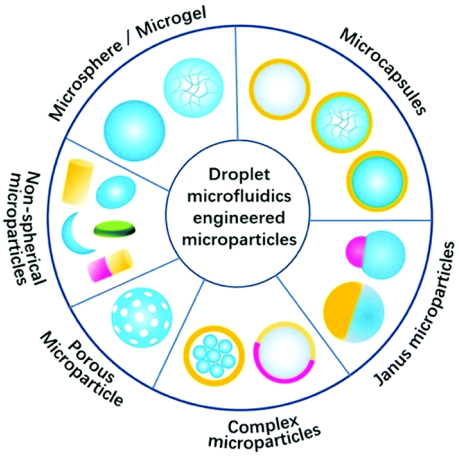

588

589 **Fig. 8:** Scheme of exemplary microparticle shapes and ultrastructures accessible by droplet-based
590 microfluidics. Republished with permission of The Royal Society of Chemistry from (Li et al., 2018) ;
591 permission conveyed through Copyright Clearance Center, Inc.

592

593 From an industrial perspective, the beauty of microfluidic fabrication is not sufficient to justify
594 the use in pharmaceutical production due to required investments and risks associated with
595 any new technology. Instead, applications requiring distinct particle properties that could not
596 be realized with other more established technologies are the most likely paths for market
597 entrance of droplet-based microfluidics in pharmaceutical carrier production (Holtze, 2013).

598 Based on the technological principles of droplet based-microfluidics, beneficial features for
599 preparing drug release systems might be:

600 *Exclusion of burst release through efficient drug embedment.* Burst release due to drug
601 molecules located at or near the particle surface is a known characteristic of several approved
602 sustained release formulations (Lundström et al., 2009) (Tunn and Wiedey, 2009), but only
603 acceptable if the drug has a broad therapeutic window. Overcoming undesired burst release
604 may allow extending the dosing intervals with a given amount of encapsulated drug and
605 broaden the spectrum of drugs applicable in microparticulate depot formulations. The burst
606 release from PLGA particles was studied with bupivacaine as a model drug used in its free
607 base form, a compound with good water solubility at neutral pH as well as in acidic
608 microenvironments (Shah and Maniar, 1993) as present in degrading PLGA particles (Ding
609 and Schwendeman, 2008). Using flow focusing microfluidics for particle preparation, a massive

610 reduction in burst release was observed compared to the batch emulsification technique due
611 to better distribution in 11 µm particles with a drug loading as high as 20 wt.% (Xu et al., 2009).

612 *Co-delivery of compounds.* The encapsulation of compounds into different compartments of
613 the same particle may be preferred over mixtures of particles loaded with either of the
614 compounds when two or more substances should be co-delivered. Examples include cases
615 where the substances are chemically incompatible, have different solubility/stability profiles or
616 time points of anticipated release, or should produce active substances or imaging probes in
617 situ, e.g., by cleavage reactions of prodrugs (Liang et al., 2015). For instance, in vaccine
618 delivery by particulate carriers, a co-delivery of adjuvant and antigen to the same cell is needed
619 (Huang et al., 2019). Furthermore, shielding encapsulated peptide from intestinal enzymes
620 may be mediated by enzyme inhibitors entrapped in an outer matrix material (Araujo et al.,
621 2015). Janus particles and other substructured particles can host substances in several
622 individual compartments as templated by microfluidic techniques (Khan et al., 2015b), which
623 can be supportive to such co-delivery concepts.

624 *Multi-step local release.* In pharmaceutical product development, simple therapeutic
625 approaches such as multiple injections are typically preferred over complex delivery systems
626 like microparticles. However, for certain sites of the body that cannot be easily reached or only
627 through interventions at risk of tissue damage, multistep release formulations may be of
628 interest, e.g., for intraoperative placement. A conventional approach would be mixtures of
629 particles with different release pattern, e.g., due to different particle sizes (Berkland et al.,
630 2001). In this regard, microfluidics could provide technical solutions by parallel channels of
631 different geometries simultaneously producing differently sized particles into one batch, thus
632 avoiding later mixing issues expected especially for small particles in dry state. Furthermore,
633 material chemistry offers a broad toolbox of stimuli-responsive materials proposed for on-
634 demand local release (Fu et al., 2018) (Bruneau et al., 2019) (Kauscher et al., 2019). While
635 many of these materials are primarily of academic interest with many questions still to be
636 addressed (safety including toxicity and long term in vivo responses, physiological relevance
637 of applied stimuli, polymer degradation/elimination, production schemes, etc.), which affects

638 the realistic chances to be translated into pharmaceutics in the next 10 to 20 years, it is still
639 relevant to evaluate the underlying principles and test their transferability to established
640 pharmaceutical additives.

641 *Sensitive compounds.* Turbulent mixing and exposure to hydrophobic interfaces can be
642 detrimental at least to some biopharmaceutics. These issues motivate the use of low-shear
643 techniques and specific environments for proteins such as present in hybrid particles from
644 hydrogels with hydrophobic membrane layers (Kong et al., 2013). Thin intermediate hydrophilic
645 layers in between a miscible dispersed phase and the continuous hydrophobic phase, as can
646 also be used to prevent premature solidification of dispersed phases by gelling agents added
647 in the continuous phase, could serve as a protective layer during microfluidic templating for
648 sensitive molecules in the dispersed phase.

649 *Patient-specific formulations for precision medicine.* The concept of dose adaptation to patient
650 needs in precision medicine can only be successful when drug formulations are available in a
651 sufficiently fine grid of doses or such doses can be rapidly produced. While feasible for
652 injections or infusions of dissolved drugs, patient-specific particulate formulations are not yet
653 established in the clinics. Microfluidics, with its given throughput, may allow preparing such
654 formulations, e.g., by microfluidic devices prefilled with a number of drugs to be chosen from
655 as needed. Existing microfluidic technologies (see e.g. Fig. 6D) may be adapted for such
656 purpose. Cancer vaccines incorporating patient materials may be another example for
657 applications with need of individualized small-batch production.

658 *Plant size reduction, workers protection and incubator technologies.* Despite investments are
659 required for setting up and validating microfluidic processes in industrial production, financial
660 aspects may be in favor of microfluidics in selected cases. For instance, when plants for small
661 batch sizes of highly toxic substances use dedicated rooms/equipment and require a relatively
662 high number of personnel for operation and process supervision due to short shifts in all-body
663 protection suits, downscaling of equipment to fit into incubators as possible for microfluidic
664 setups may substantially reduce overall costs.

4.1 Preparation of particles from preformed polymers

The preparation of drug loaded particles through emulsion techniques is well established for hydrophobic and hydrophilic bioactive compounds by batch processes (Wischke and Schwendeman, 2008). Most commonly, hydrophobic polymers such as PLGA serve as matrix materials, which are dissolved in an organic solvent (o-phase) like dichloromethane or ethyl acetate having a limited solubility in an aqueous phase (w-phase). Hydrophobic drugs can be co-dissolved or dispersed in the o-phase, which is then emulsified in the w-phase forming an o/w emulsion. The slow extraction of the o-phase solvent into the w-phase, from where it may evaporate, results in shrinkage of nascent particles and eventually their solidification. For a hydrophilic payload, an additional w_1 phase is very commonly used to form $w_1/o/w_2$ double emulsions. The emulsification and solvent extraction/evaporation process has been realized for a number of (model) compounds in microfluidic channels. Based on the increasing availability of ready to use microfluidic equipment packages and available technical application notes, more studies are expected to be published for various drugs encapsulated into preformed polymers by microfluidic techniques in the next couple of years. Computational tools, including fluid dynamics simulation, have also been successful to predict droplet and polymer particle sizes under variation of flow conditions (Vladisavljevic et al., 2014), thus supporting efficient research and development.

As some channel materials such as PDMS tend to swell in organic solvents resulting in channel diameter alteration with time, o-phase solvents have been exchanged, e.g., to dimethyl carbonate (Hung et al., 2010). Alternatively, solvent resistant glass, steel, or silicon devices have been used (Herranz-Blanco et al., 2017) (Ofner et al., 2017) (Yadavali et al., 2018). Given the permeability of PDMS to dimethyl carbonate and the high surface to volume ratio of microfluidic channels, on-chip solvent extraction/evaporation has been reported (Hung et al., 2010). For devices with non-permeable channel walls, particles can be collected in an open vessel for solvent evaporation or commercially available membrane modules may be integrated in the devices for solvent exchange in cross-flow.

693 Bulk emulsification techniques for drug encapsulation in hydrophobic polymers are often linked
694 to a number of critical issues, e.g., a potential drug instability at interfaces during shear-based
695 emulsification, drug loss to the continuous water phase, improper encapsulation as
696 characterized by drug molecules being deposited in larger aggregates at or near the particle
697 surface, drug instability during storage, and release pattern with high initial rates (burst) and/or
698 incomplete release. Microfluidic techniques could address at least some of these points so far.
699 As noted above, the massive burst release of bupivacaine from conventionally prepared
700 ~11 µm or ~44 µm PLGA particles could be overcome by microfluidic preparation with a more
701 homogeneous drug entrapment in the particle core. In this context, another relevant feature
702 may be the much more homogeneous particle size (Fig. 9A) (Xu et al., 2009), thus avoiding a
703 fine particle fraction with higher surface to volume ratio contributing to faster release. Similar
704 observations were made for encapsulation of Ciclosporin A in 5-10 µm PLGA particles
705 comparing o/w microfluidic emulsification to spray drying and bulk emulsion/solvent
706 evaporation, where encapsulation efficiencies were much higher and release was more
707 prolonged for particles from microfluidics (Keohane et al., 2014).

708 While water can generally penetrate into compact PLGA particles at a given rate, the exchange
709 of water and drug under release conditions can be accelerated by introducing pores, e.g., by
710 adding salt to the w_1 phase serving as osmotic agent during particle formation (Wischke et al.,
711 2010). Accordingly, ammonium carbonate as porogen allowed for a faster but still controlled
712 release of a dye, coumarin-6, from ~90 µm PLGA particles from microfluidic production
713 (Amoyav and Benny, 2019). Exchanging PLGA with PEG-PLGA resulted in massively
714 accelerated burst-like release of Cyclosporine A due to high microparticle porosity and rapid
715 water uptake under release conditions as promoted by domains from hydrophilic PEG chains
716 (Keohane et al., 2014). Furthermore, (open) pores can be introduced by using w/o/w rather
717 than o/w emulsions, which may have contributed to the observed ~30% burst release of well
718 water-soluble lidocaine hydrochloride from porous PCL particles (Vladisavljevic et al., 2014).

719 Encapsulation efficiency is a very relevant feature in particle production and is linked to both
720 the formulation approach and the characteristics of the employed substances. A number of

721 drugs were investigated for microfluidic encapsulation in polyesters, including, e.g., paclitaxel
722 (He et al., 2011), enoxacin (Kim et al., 2013a), risperidone (Jafarifar et al., 2017), latanoprost
723 and dexamethasone (Leon et al., 2015). Other than in large stirred vessels, only a relatively
724 small volume of continuous phase is in contact with the nascent particles within the
725 confinement of a microfluidic channel. Therefore, only this fluid volume may account for
726 exchange processes with the o-phase, namely solvent extraction for particle hardening and
727 drug loss by diffusion and/or convective forces. For size ratios of droplet-to-channel width of
728 <0.8, the mass transfer of dimethyl carbonate into water in an o/w two-phase system was
729 dominated by diffusion (Vasiliauskas et al., 2015). Generally, hydrophobic drugs often have
730 high encapsulation efficiencies in bulk o/w emulsions, which should also transfer to
731 microfluidics. As expected, for very poorly water-soluble anticancer and antiinflammatory drugs
732 like sorafenib and celecoxib, a quantitative encapsulation in microparticles from acetalated
733 dextran was observed at least when the polymer was used above a certain threshold
734 concentration. It was concluded that the polymer accumulates at the interface and serves as
735 diffusion barrier during droplet shrinkage and particle solidification (Vasiliauskas et al., 2015).
736 While more studies on the balance of solidification speed and drug leakage in microfluidic
737 channels are still to be conducted, including model studies in zero-flow conditions for
738 determining diffusion coefficients (Kinoshita et al., 2016), it is obvious that the
739 solubility/miscibility of the o-phase solvent in the water phase can mediate drug loss due to
740 instable droplet interfaces and solubility enhancement.

741 Dimethyl sulfoxide/dimethyl carbonate as a mixed o-phase for PLGA were emulsified in the
742 jetting regime into small droplets, from which the solvents were subsequently extracted leading
743 to the formation of numerous nanoparticles through a proposed diffusion-limited cluster
744 aggregation mechanism (Xu et al., 2017a). At achieved drug payloads of >15 wt.%, the
745 encapsulation efficiencies by this technique were up to 88% for hydrophobic tamoxifen and
746 80% for hydrophilic doxorubicin, which were 20% higher than for doxorubicin loaded particles
747 formed by nanoprecipitation. Furthermore, better entrapment of doxorubicin within the polymer

matrix material could be concluded for particles from those solvent mixtures based on their substantially slower release (Fig. 9B) (Xu et al., 2017a).

The encapsulation of hydrophilic substances such as proteins is typically conducted by w/o/w emulsion, where – by concept – microfluidics provide much higher precision of entrapment than bulk double emulsification. In particular, bulk double emulsions may regularly be associated with fusion of w_1 and w_2 phase droplets during high shear emulsification of the w_1/o primary emulsion in the continuous w_2 phase. By microfluidic double emulsion, successful protein encapsulation has been demonstrated for PCL (Pessi et al., 2014) or PLA particles (Bokharaei et al., 2017) at least with bovine serum albumin as a relatively stable model protein. Encapsulation efficiencies of 84% and a distinct burst release were observed (Pessi et al., 2014). However, there might be a lack of subsequent protein release from polyester matrices as can be expected by restricted protein diffusion in hydrophobic polymers and potentially protein unfolding phenomena. Employing very thin hydrophobic polymer shells as membranes around a liquid core may reduce the diffusion length through the polymer phase and allow controlling the release of hydrophilic molecules. Such thin-shell (70 – 150 nm) semipermeable capsules from high molecular weight PLGA templated by w/o/w emulsions released hydrophilic dyes in vitro and in vivo over several weeks. In addition to dye diffusion and polymer degradation, the mechanical failure of the thin shell under mechanical stress during injection and in the tissue may have had a major contribution to release (Lee et al., 2017).

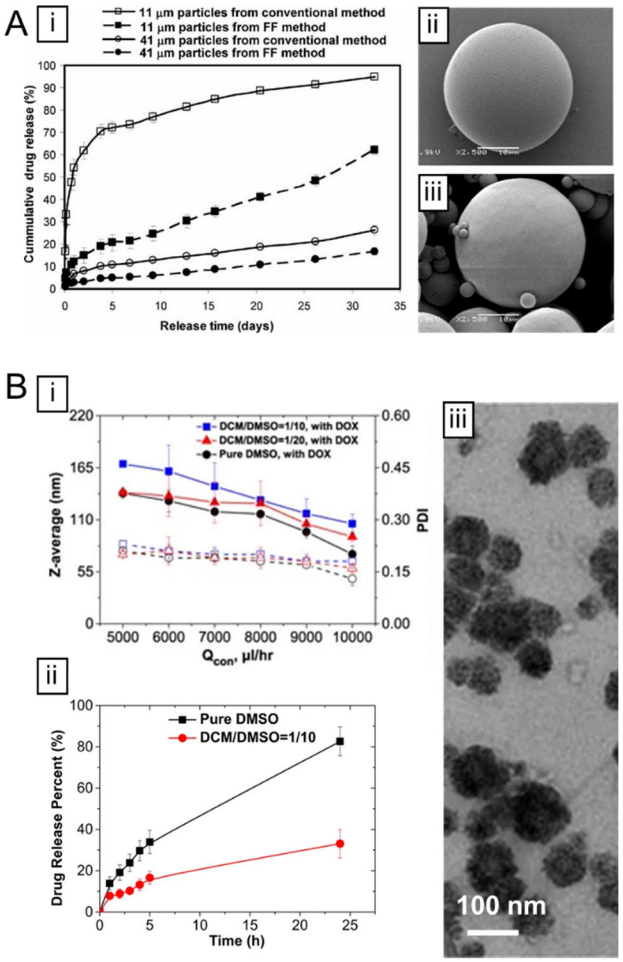

Fig. 9: Release characteristics of drug loaded PLGA particles. (A) Bupivacaine loaded particles. (i) Release pattern with reduction of burst release by microfluidic preparation (FF: micropluidic flow focusing). (ii, iii) SEM images indicating particle surface structure and size distribution (mean ~11 μm) for particles from microfluidic preparation (ii) compared to conventional bulk emulsification technique (iii). Reproduced with permission from (Xu et al., 2009) Copyright © 2009 Wiley-VCH Verlag GmbH & Co. KGaA, Weinheim. (B) Doxorubicin loaded nanoparticles prepared by mixed o-phase solvents. (i) particle size distribution depending on flow rate of continuous water phase (flow rate of dispersed phase 50 μl/min), (ii) doxorubicin release depending on solvents used for preparation, (iii) TEM image of PLGA particles with black spots assigned as doxorubicin aggregates. Adapted from (Xu et al., 2017a) under a Creative Commons Attribution 4.0 International License (https://creativecommons.org/licenses/by/4.0/).

Beside hydrophobic polymers, also preformed hydrophilic polymers can be dispersed into droplets by microfluidics. In order to stabilize the dispersed phase droplets, chemical crosslinking is often used as main stabilization principle, as addressed in section 4.2. However, also physical interactions such as complexation or temperature-induced gelation are common principles in such hydrogel particles, also termed as microgels. Furthermore, the clustering of hydrophobic chain segments of amphiphilic polymers into bridged micelles can be used to

785 build physical netpoints in microgels (Wang et al., 2013). A typical material to prepare
786 microgels via physical interaction is alginate. It gels by complexation of divalent cations like
787 Ca^{2+}, which are added on the chip either directly as a calcium chloride solution during droplet
788 templating or by ligand exchange through an additional aqueous phase (Mazutis et al., 2015)
789 (Hati et al., 2016). Alternatively, calcium ions are often provided to previously templated
790 droplets in the collection bath (Chuah et al., 2009) (Hou et al., 2019). Model proteins or
791 antibodies codissolved in the alginate solution have been encapsulated in the hydrogel phase
792 by this procedure (Hati et al., 2016), or separate protein and alginate phases allowed liquid
793 core enclosure by the alginate hydrogel (Yu et al., 2019). In a typical setting, laborious removal
794 of the continuous oil phase is required prior to further use.

795 Also hybrid particles from preformed polymers have been prepared with hydrophobic cores
796 and hydrophilic shells (Wu et al., 2013) or vice versa (Kong et al., 2013), where the different
797 compartments can act as depots, release rate controlling units, or both.

798

799 ***4.2 Drops as microreactors for polymer (network) synthesis***

800 Droplets are transported in microchannels in a synchronized manner in one plane. Based on
801 this feature, they are accessible to various types of subsequent modifications, e.g.,
802 deformation, splitting, fusion, liquid injection, mixing, or illumination. Using the tool box of
803 materials chemistry, droplets can serve as microreactors for transforming
804 monomers/oligomers into polymers, particularly polymer networks, in order to adapt and
805 maintain a desired particulate structure and shape. In this way, particles with various material
806 properties can be made available, e.g., by systematically changing the flow rates of
807 comonomer phases and thus the copolymer composition during screening experiments.
808 Furthermore, as bulk polymer network materials cannot be easily processed into micrometer-
809 sized particles with defined shapes at a relevant throughput, in situ crosslinking of droplets for
810 network formation is the way of choice for such materials. For pharmaceutical applications, the
811 level of (chemical) homogeneity of the material, the structure of netpoints, the degradability of
812 the polymer network, the nature of degradation products, and the potential interference of

crosslinking reactions with simultaneously present drug molecules are, however, subjects requiring particular attention when following this path.

Microgels, i.e. microparticulate hydrogel networks, are commonly obtained by in situ polymer network synthesis, most often via photoinduced radical polymerization of (meth)acrylate moieties (Plamper and Richtering, 2017). Such concepts can also be transferred to microfluidics. The heat generated during photoinitiated free radical polymerization of tripropylene glycol diacrylate precursors in the presence of a catalyst could also be used to induce a second catalyzed polymerization, eventually resulting in an interpenetrating network of polyacrylate and polyurethane/urea (Li et al., 2008a). Further crosslinking concepts explored for microfluidic microgel fabrication include Schiff bases formed between aldehyde and amine moieties of polysaccharides (Zhang et al., 2011), crosslinking of polyethylenimine with diisocyanates by an addition reaction (Polenz et al., 2015), or horseradish peroxidase catalyzed gelation of tyramine functionalized gelatin used in mixture with agarose as a thermogelling material (Chau et al., 2014). In the latter case, the enzyme induces gelation by conversion of tyramine to phenoxy radicals that are known to couple through radical reactions (Sakai and Nakahata, 2017), eventually resulting in complex structured agarose-gelatin networks with controllable mechanical stiffness (Fig. 10A) (Chau et al., 2014). If radical polymerization should be avoided, photoinduced 2+2 cycloaddition reactions of cinnamylidene acetic acid (CAA) moieties may be employed to create netpoints. In this study, an o/w emulsion of PEG-CAA dissolved in $CHCl_3$ was exposed to UV irradiation at 308 nm, followed by solvent exchange with water to obtain stable microgels (Fig. 10B). By irradiation conducted for increasing time periods without the presence of photoinitiators, the network density and thus the mesh size could be controlled (Tuncaboylu et al., 2017), which might allow controlling drug release rates. When chain segments, which are subject to a reversible hydration at a lower critical solution temperature like poly(*N*-isopropylacrylamide), are incorporated in microgels constructed e.g. by azide-alkyne click reaction, size expandable particles can be obtained (Fig 10C) (Hackelbusch et al., 2015).

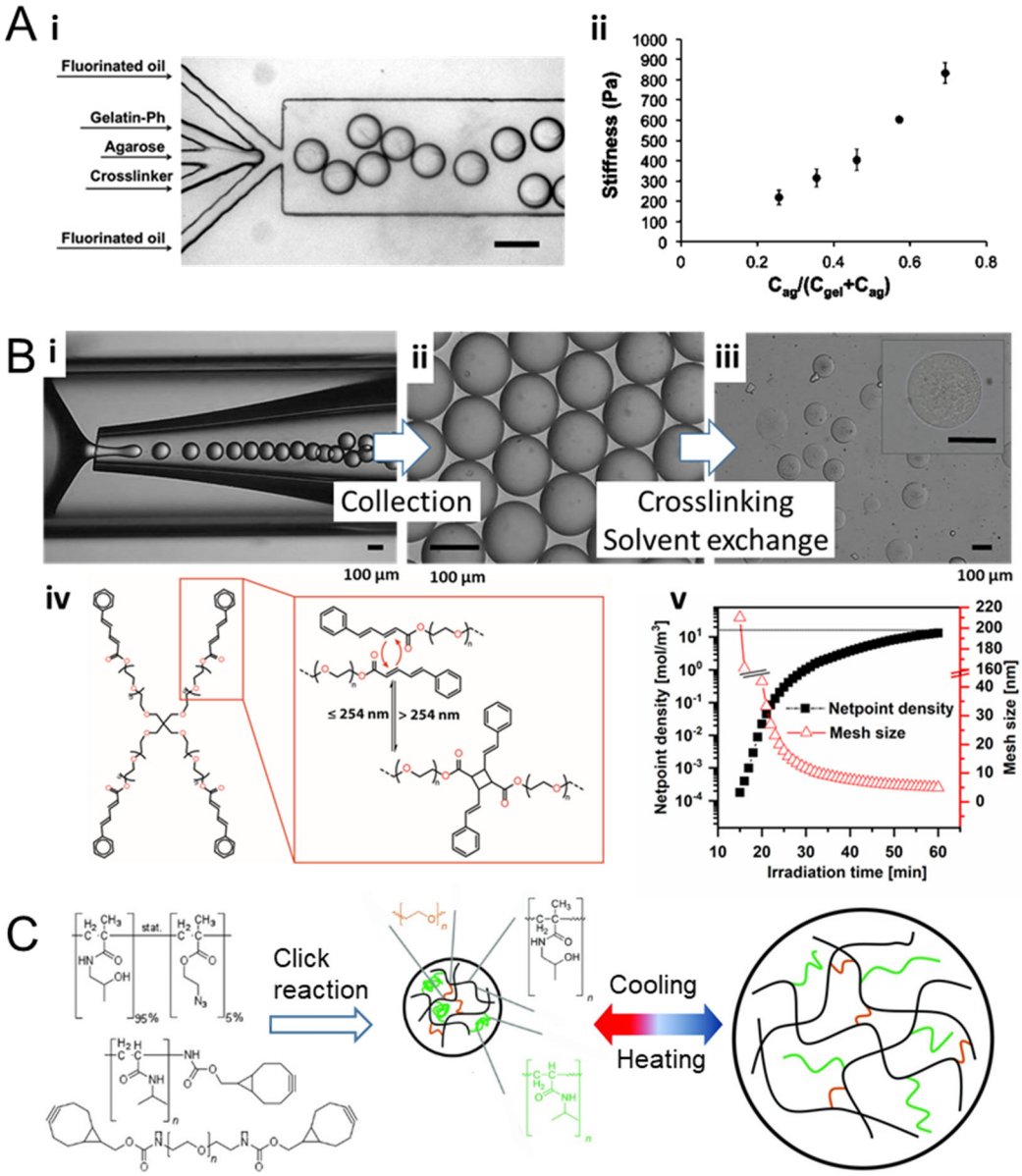

Fig.10: Microgel synthesis by polymerization/crosslinking reactions in template droplets. (A) Enzymatic crosslinking by horseradish peroxidase. (i) Templating w/o droplets from agarose, tyramine functionalized gelatin, and HRP plus hydrogel peroxide. (ii) Effect of agarose to gelatin ratio on microgel stiffness. Adapted with permission from (Chau et al., 2014). Copyright (2014) American Chemical Society. (B) Photoinduced 2+2 cycloaddition reaction. (i) o/w droplet templating; star shaped PEG bearing CAA moieties dissolved in $CHCl_3$ serves as dispersed phase, (ii) particle collection in aqueous poly(vinyl alcohol) in a sealed chamber, (iii) microgel particles after crosslinking and evaporation of $CHCl_3$ resulting in solvent exchange with water, (iv) principle of 2+2 cycloaddition reaction, (v) Effect of irradiation time at 308 nm on polymer network properties. Reprinted from (Tuncaboylu et al., 2017) with permission from Elsevier. (C) Preparation of thermosensitive microgels containing temperature-responsive poly(*N*-isopropylacrylamide) segments by strain promoted azide-alkyne cycloaddition reaction, an example of click chemistry. Adapted with permission from (Hackelbusch et al., 2015); © 2015 WILEY‐VCH Verlag GmbH & Co. KGaA, Weinheim.

The release of substances from microgels by diffusion may be rate controlled by the polymer network density (Klinger and Landfester, 2012). For instance, bevacizumab, a therapeutic antibody for cancer therapy, could be released from PEG-based microgels prepared by thiol-en click chemistry with an apparent correlation of release rate and microgel mesh sizes (Gregoritza et al., 2018). Moreover, it may also be possible to slowly release substances with hydrodynamic diameters larger than the nominal average mesh size of the network considering the high mobility of hydrated polymer chain segments and common network inhomogeneity.

In hybrid microgels, features contributed by their components can be combined. Liposomes added to the microgel-forming dispersed phase prior to crosslinking offer opportunities to buffer rapid release of hydrophilic drugs by incorporation in the liposome core. Furthermore, liposomes allowed the loading of microgels with hydrophobic compounds by solubilization in the double layer of liposomes (Jeong et al., 2014).

In addition to the use of drug-compatible crosslinking strategies, the payload may be incorporated after network formation by diffusion, e.g., by soaking microgels in drug solution. Apparently, when drug easily diffuses into the microgel during loading, the gel presents a limited diffusion barrier only and drug release will be relatively fast if no binding motives exist inside the gel. Therefore, coating strategies for hydrogels, as also applicable on the macroscale (Wischke et al., 2013), might allow to hinder the immediate release of hydrophilic compounds from microgels. For instance, this concept was explored by covering anionic hyaluronic acid-based microgels with cationic poly(*L*-lysine) after protein loading (Labie et al., 2019).

Switchable swelling is another main principle to rate drug release from microgels. Through, e.g., temperature- or pH-induced increase of microgel hydration, diffusivity and thus release of incorporated substances may be triggered at the time of interest (Klinger and Landfester, 2012) (Agrawal and Agrawal, 2018). However, when inducing microgel shrinkage to switch-off the release, an outwards directed fluid flow might temporarily boost release if no additional principles of drug retention such as ionic interactions with the gel matrix or covalent drug binding are implemented.

884 Beside hydrophilic polymers, also hydrophobic materials can be of interest to synthesize
885 network materials in microfluidic droplets. Such micronetwork particles, possessing a thermal
886 transition (e.g. a melting transition) above body temperature, may be deformed above this
887 temperature and fixed in the shape of interest through the shape-memory effect (Friess et al.,
888 2014). By microfluidic templating and subsequent crosslinking of PCL-based micronetworks,
889 spherical monodisperse particles were produced that could be loaded by swelling with
890 hydrophobic model compounds. The monodisperse particles could subsequently be
891 transformed and fixed as prolate ellipsoids of various aspect ratios, all originating from the
892 same mother particles for best comparability. Those micronetworks were used to explore
893 shape, size, and time dependency of phagocytic uptake, which is of interest for intracellular
894 delivery (Friess et al., 2019).
895
896 **4.2 Particle designs with complex structures**
897 The ability of microfluidic devices to dose defined quantities of liquids into or aside of each
898 other and subsequently apply manipulation including externally triggered crosslinking opens a
899 wide field of possible particle (sub)structures, e.g., different shapes, compartments, local
900 physicochemical properties of particles as well as payloads. Most prominent are Janus
901 particles, which contain at least two hemispheres with distinctly different properties such as
902 different matrix materials or different payloads. Such particles can be prepared by coaxial flow
903 of two inner phases injected side-by-side into one outer phase, where they are immediately
904 stabilized, e.g., by crosslinking. The volume ratio of the dispersed phases, the time until
905 crosslinking, and the presence of surfactants can be critical when building Janus particles from
906 two distinctly different immiscible materials, as they may undergo a transition towards a
907 capsule-like shape driven by reduction of interfacial energies (Khan et al., 2014). When the
908 two hemispheres should be composed of distinctly different materials, sufficient adhesion
909 between the half-spheres can also become a critical issue.

910 As an alternative to side-by-side injection of the dispersed phases, Janus particles can be
911 obtained through manipulation and/or phase separation of single or double emulsions, i.e.,

912 starting from an initially concentric arrangement. In this case, geometric assistance can be
913 provided by collection channels with a smaller height than the diameter of double emulsion
914 droplets resulting in droplet squeezing and stretching. The resulting viscous friction induced a
915 dislocation of the inner droplet of the double emulsion to the end of the plug of the middle
916 phase, in which the particle shape could be fixed by online UV irradiation associated with matrix
917 material polymerization (Chen et al., 2009).

918 Other concepts rely on phase separation, e.g., starting from co-dissolved polymers in single
919 emulsion droplets, which continuously phase separate when the solvent is extracted. In such
920 processes, the nature and concentration of polymer, solvent, and surfactants are of high
921 relevance, as they define the interfacial tensions between the two different polymer-rich
922 phases and the continuous phase. In case of resulting negative spreading parameters, both
923 dispersed polymer-rich phases can undergo dewetting and minimize their surface-to-volume
924 ratio by forming half spheres. Depending on the precipitation kinetics of the two materials, a
925 full phase separation of the two initially co-dissolved materials to Janus particles has been
926 observed, e.g., for PLA-polystyrene model systems (Min et al., 2014). For phase separation of
927 PLGA/PCL mixtures from o/w emulsions, the o-phase solvent was demonstrated to massively
928 affect spreading parameters and thus particle characteristics. While dimethyl carbonate
929 resulted in Janus particles at all PLGA/PCL ratios due to always negative spreading
930 parameters of the polymer phases, dichloromethane produced PCL-PLGA core-shell or golf-
931 ball like particles due to preferential wetting of the PLGA phase (Fig. 11A) (Cao et al., 2015).

932 Particles with characteristic anisotropic shapes can also be obtained from double emulsions
933 with several inner phase droplets. These inner phase droplets can serve as a mask over which
934 a thin polymer layer is stretched after crosslinking of low-concentration solutions of polymer
935 precursors in the middle phase and subsequent solvent extraction. When one microgel (m)
936 particle and one oil droplet were co-encapsulated in $(m+o_1)/w/o_2$ double emulsions with a
937 relatively low volume of the w-phase, the immiscible inner phase objects (m, o_1) were located
938 next to each other and could slightly deform the w-phase droplet (Fig. 11B). The w and the o_2

phases can then be simultaneously solidified by acrylate chemistry, leading to marked anisotropic particle shapes after drying (Thiele and Seiffert, 2011).

A partial coalescence of several inner phase droplets from identical materials in double/multiple phase emulsions may occur depending on the quality of their interface stabilization. This coalescence may be time-dependent statistic events, thus requiring immediate fixation of a desired intermediate shape by a fast middle phase polymerization. Alternatively, coalescence may be controllable with relatively stable intermediate states , which supports to obtain well-defined geometries in a reproducible manner. Such states were realized for Pickering emulsions due to jamming of nanoparticulate stabilizers at the interfaces of coalescing inner phase droplets (Studart et al., 2009). An arrested coalescence was also reported for $o_1/o_2/w$ double emulsions containing an o_1-phase from ionic liquids and salt as osmotically active agent. The diffusion of water into the o_1 phase eventually led to a $w/o_1/o_2/w$ system. An intermediate state with a stability over several days is adapted after partial coalescence of the o_1 phases within each o_2 droplet, allowing crosslinking of the o_1 phase by acrylate chemistry (Fig. 11C) (Feng et al., 2019).

Stop-flow microfluidics is an alternative technique to produce various particle shapes. It differs from droplet-based microfluidics by (i) operating commonly with the flow of one single phase fluid that (ii) is repetitively stopped for channel illumination through a mask defining the volume accessible for polymerization (Bong et al., 2014). Pulsed-laser illumination can also be applied in droplet-based microfluidics at the collection channel (Krüger et al., 2019), thus defining the portion of droplets/plugs that will be solidified. This technique, however, demands a perfect synchronization of drop formation/passage rate and laser pulses in the illumination area and an extremely fast polymerization for reproducible particle shapes.

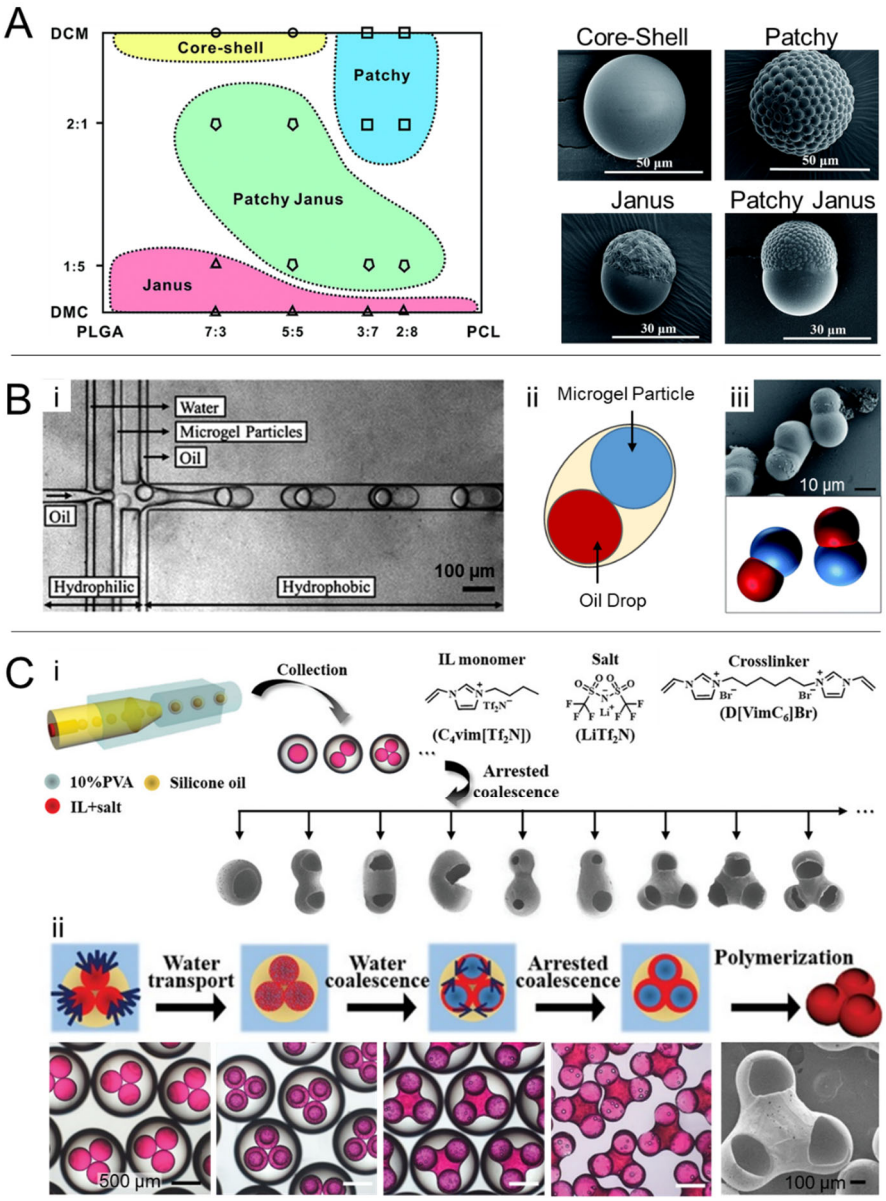

Fig.11: Designing complex shape particles from droplets template by microfluidics. (A) Phase separation of o-phases during solvent extraction from o/w single emulsion droplets containing co-dissolved PCL and PLGA at different ratios, resulting in different shapes including Janus particles depending on the employed solvent and PLGA/PCL ratio. Republished with permission of The Royal Society of Chemistry from (Cao et al., 2015); permission conveyed through Copyright Clearance Center, Inc. (B) Janus particls formation by co-injection of oil phase and microgel (m) particles in $(m+o_1)/w/o_2$ double emulsions. (i) Experimental setup. (ii) Scheme of double emulsion droplet containing one microgel particle and one oil droplet. (iii) Images and cartoon of dried Janus particles after o_1 and w-phase polymerization. Republished with permission of The Royal Society of Chemistry from (Thiele and Seiffert, 2011); permission conveyed through Copyright Clearance Center, Inc. (C) Multi-unit particles formed by arrested coagulation and crosslinking of ionic liquid phase (o_1) after salt-induced water penetration into o_1. (i) Scheme of emulsification and reagents employed in o_1 phase. (ii) Range of possible particle shapes. (iii) Exemplary procedure to produce triple-core particles. Adapted with permission from (Feng et al., 2019) © 2019 WILEY-VCH Verlag GmbH & Co. KGaA, Weinheim.

The preparation of double emulsions by microfluidics offers the opportunity to incorporate several inner-phase droplets per particle (compare Fig. 11). For incorporation of a pharmaceutical compound, this may be advantageous as unintentional damage of one inner-phase compartment during particle handling or application would not necessarily result in leakage of the entire payload of the particle. At the same time, the production of multi-core double emulsions is linked to specific demands regarding flow conditions and device geometries. Two-step devices, where the orifices for the first and second emulsification ($w_1/o/_2$) were spatially separated and followed one after the other, had the advantage of only minor impact of w_1 flow on the sizing of o-phase droplets (Shao et al., 2013). By adjusting flow rates and thus controlling the capillary numbers for producing $w_1/o/w_2$ emulsions, a transition in encapsulation from one to six to one droplet(s) could be observed when increasing the w_1 flow rate, while transition regions produced fluctuating numbers of w_1 droplets (Fig 12 A) (Nabavi et al., 2017b).

Multiple inner phase compartments can also be produced inside each other leading to higher order core shell structures. When thin shell capsule-in-capsule PLA particles were formed from $w_1/o_1/w_2/o_2/w_3$ quadruple emulsions, the payload of the w_1 and w_2 phases could be consecutively released in accelerated PLA degradation experiments or through osmotic pressure induced capsule wall rupture (Fig. 12B) (Lee et al., 2018). Another concept presented two identical hydrophilic phases each containing a different protein payload. To obtain such particles without mixing of the two dispersed phases, one protein loaded PEG-DA droplet was first prepared and crosslinked followed by injection and fusion with a second protein loaded droplet, which again was crosslinked by UV irradiation (Fig. 12C). Despite intended by the authors for a use as synthetic cells comprising two enzymes in different hydrogel compartments, the concept may be applicable also to pharmaceutics as a slow protein release from the gel has been observed (Tan et al., 2017). Alternatively, such constructs might, in the future, be considered for in situ on-demand synthesis of bioactive molecules in the body by an enzymatic cascade.

By loading microparticles with colloidal particles, either as filler component or with incorporated drug, composite particles can be obtained. PLGA particles (45 µm) containing dispersed nanoclay showed a slower paracetamol release compared to particles without filler as assigned to enhanced particle density and drug diffusion path length, while this effect was less prominent for 17 µm PLGA particles (Fig. 12D) (Ekanem et al., 2015). Microgel particles incorporating ketoprofen loaded polyacrylate nanoparticles have been prepared by coupling a micromixer for nanoemulsion preparation with a coaxial microfluidic device for microgel templating followed by simultaneous UV crosslinking. In this case, the drug loaded nanoparticles could liberate from the covalently crosslinked microgel with time (Khan et al., 2015). A release of nanoparticles from Janus microgel particles has also been reported by disintegration of physical crosslinks in response to temperature and/or pH changes (Chen et al., 2013). Overall, by complex particle designs, a number of release principles may become accessible that add to the most common diffusion-based release of single compounds from particulate carriers.

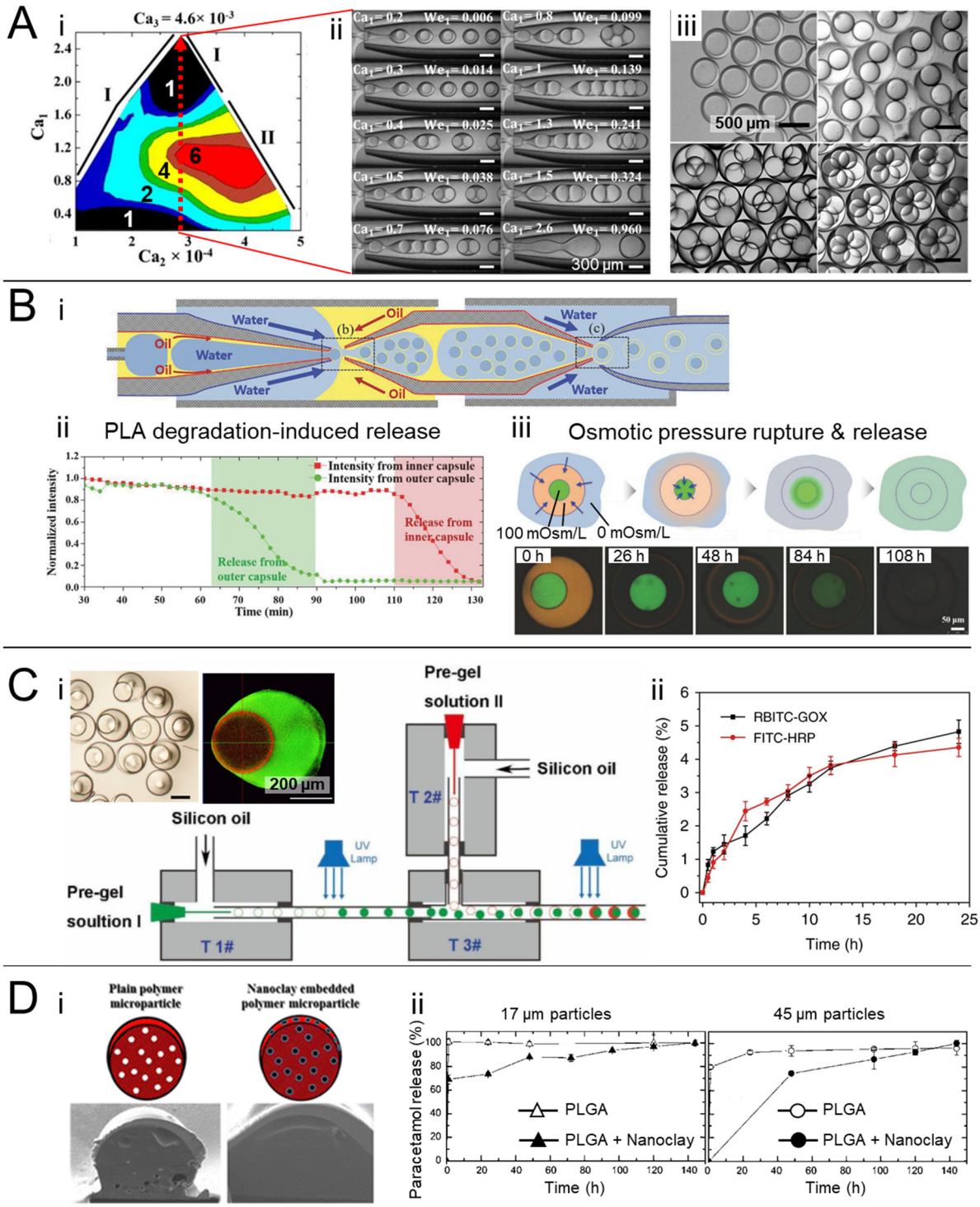

Fig.12: Concepts for drug incorporation and release in multi-compartment particles. (A) Tuning numbers of encapsulated droplets in $w_1/o/w_2$ emulsions. (i) Color map correlating Ca_1 (w_1 phase) and Ca_2 (o-phase) at constant Ca_3 (w_2 phase) with the number of formed inner phase droplets. Non-marked regions are transition regions where fluctuating numbers of droplets have been encapsulated. (ii, iii) Images of droplet pinch-off and final emulsion. Adapted from (Nabavi et al., 2017b) under a Creative Commons Attribution 4.0 International License (https://creativecommons.org/licenses/by/4.0/). (B) Capsule-in-capsule PLA particles. (i) Formation of w/o/w/o/w quadruple template emulsion. (ii) Consecutive release of two dyes from the outer and inner capsule in accelerated degradation condition (basic methanol solution). (iii) Loading both capsule cores with salt (100 mOsm/l) and placing them in distilled water caused water influx

(blue arrows) and cracking of capsule walls facilitating dye release by osmotic triggers. Adapted with permission from (Lee et al., 2018) © 2018 WILEY-VCH Verlag GmbH & Co. KGaA, Weinheim. (C) Double compartment PEG-based hydrogel particles with protein payload. (i) Optical and fluorescence microscopic images. (ii) Preparation scheme with droplet injection and crosslinking. The second inner phase droplet fuses with the presolidified first inner phase droplet. (iii) Release of dye-labeled glucose oxidase (GOX) and horseradish peroxidase (HRP). Reproduced from (Tan et al., 2017) under a Creative Commons Attribution 4.0 International License (https://creativecommons.org/licenses/by/4.0/). (D) Composite PLGA particles with 2 wt.% incorporated nanoclay (plate-like montmorillonite). (i) Scheme and SEM images of particles with reduced porosity. (ii) Paracetamol release for 17 µm and 45 µm particles with or without nanoclay filler. Adapted with permission from (Ekanem et al., 2015), Copyright (2015) American Chemical Society.

Conclusions

Droplet-based microfluidic techniques represent a continuously growing field, where many fundamental principles have been established that now can facilitate the efficient preparation of functional polymer particles. As instrumentation for microfluidics and technical services in chip manufacturing became increasingly available, it can be expected that droplet-based microfluidics will continue to attract more scientists that aim at encapsulating drug molecules into tailor-made polymeric carriers.

For some of the potential beneficial features (compare section 4) that microfluidic manufacturing may have for the preparation of drug carriers, some pieces of literature already indicate that this technology may meet the described expectations. For some of the other proposed points, including shear sensitive compound encapsulation and multi-step local release, experimental proof demonstrating advantages of microfluidic processing is still to come.

The use of droplet-based microfluidics in pharmaceutics will, despite the availability of far progressed methodologies to increase throughput, likely not be in mass products with tons of annual sales. Instead, high value products, presumably with small batch sizes might be a more likely scenario. Given the possibility for aseptic manufacturing and the beneficial feature of microfluidics to allow handling of small volumes, possible applications in pharmaceutics may be found in precision medicine. Examples may be particles incorporating patient material, such as for cancer vaccination, or the use of prefilled microfluidic devices by which the quantity of

encapsulated doses for slow-release formulations or on-demand release systems may be individually defined based on patient-specific needs.

Acknowledgements

The authors of (Lashkaripour et al., 2019) are acknowledged for providing a high resolution version of their published figure used as basis for Fig. 2. This work was financially supported by the Helmholtz Association through program-oriented funding.

References

Abate, A.R., Kutsovsky, M., Seiffert, S., Windbergs, M., Pinto, L.F.V., Rotem, A., Utada, A.S., Weitz, D.A., 2011. Synthesis of Monodisperse Microparticles from Non-Newtonian Polymer Solutions with Microfluidic Devices. Adv. Mater. 23, 1757-1760.

Abate, A.R., Weitz, D.A., 2011. Faster multiple emulsification with drop splitting. Lab Chip 11, 1911-1915.

Agrawal, G., Agrawal, R., 2018. Functional Microgels: Recent Advances in Their Biomedical Applications. Small 14, 1801724.

Alkayyali, T., Cameron, T., Haltli, B., Kerr, R.G., Ahmadi, A., 2019. Microfluidic and cross-linking methods for encapsulation of living cells and bacteria - A review. Anal. Chim. Acta 1053, 1-21.

Amoyav, B., Benny, O., 2019. Microfluidic Based Fabrication and Characterization of Highly Porous Polymeric Microspheres. Polymers 11, 419.

Amstad, E., Chemama, M., Eggersdorfer, M., Arriaga, L.R., Brenner, M.P., Weitz, D.A., 2016. Robust scalable high throughput production of monodisperse drops. Lab Chip 16, 4163-4172.

Amstad, E., Datta, S.S., Weitz, D.A., 2014. The microfluidic post-array device: high throughput production of single emulsion drops. Lab Chip 14, 705-709.

Amstad, E., Gopinadhan, M., Holtze, C., Osuji, C.O., Brenner, M.P., Spaepen, F., Weitz, D.A., 2015. Production of amorphous nanoparticles by supersonic spray-drying with a microfluidic nebulator. Science 349, 956-960.

Amstad, E., Weitz, D.A., 2017. Reply to the 'Comment on "Robust scalable high throughput production of monodisperse drops"' by M. Nakajima, Lab Chip, 2017, 17, DOI: 10.1039/C7LC00181A. Lab Chip 17, 2332-2333.

Araujo, F., Shrestha, N., Shahbazi, M.A., Liu, D.F., Herranz-Blanco, B., Makila, E.M., Salonen, J.J., Hirvonen, J.T., Granja, P.L., Sarmento, B., Santos, H.A., 2015. Microfluidic Assembly of a Multifunctional Tailorable Composite System Designed for Site Specific Combined Oral Delivery of Peptide Drugs. ACS Nano 9, 8291-8302.

Barbier, V., Willaime, H., Tabeling, P., Jousse, F., 2006. Producing droplets in parallel microfluidic systems. Phys. Rev. E 74, 046306.

Benson, B.R., Stone, H.A., Prud'homme, R.K., 2013. An "off-the-shelf" capillary microfluidic device that enables tuning of the droplet breakup regime at constant flow rates. Lab Chip 13, 4507-4511.

Berkland, C., Kim, K.K., Pack, D.W., 2001. Fabrication of PLG microspheres with precisely controlled and monodisperse size distributions. J. Controlled Release 73, 59-74.

Bokharaei, M., Saatchi, K., Hafeli, U.O., 2017. A single microfluidic chip with dual surface properties for protein drug delivery. Int. J. Pharm. 521, 84-91.

Bong, K.W., Lee, J., Doyle, P.S., 2014. Stop flow lithography in perfluoropolyether (PFPE) microfluidic channels. Lab Chip 14, 4680-4687.

Bruneau, M., Bennici, S., Brendle, J., Dutournie, P., Limousy, L., Pluchon, S., 2019. Systems for stimuli-controlled release: Materials and applications. J. Controlled Release 294, 355-371.

Cao, X.D., Li, W.X., Ma, T., Dong, H., 2015. One-step fabrication of polymeric hybrid particles with core-shell, patchy, patchy Janus and Janus architectures via a microfluidic-assisted phase separation process. RSC Adv. 5, 79969-79975.

Chau, M., Abolhasani, M., Therien-Aubin, H., Li, Y., Wang, Y.H., Velasco, D., Tumarkin, E., Ramachandran, A., Kumacheva, E., 2014. Microfluidic Generation of Composite Biopolymer Microgels with Tunable Compositions and Mechanical Properties. Biomacromolecules 15, 2419-2425.

Chen, C.H., Shah, R.K., Abate, A.R., Weitz, D.A., 2009. Janus Particles Templated from Double Emulsion Droplets Generated Using Mcrofluidics. Langmuir 25, 4320-4323.

Chen, Y.H., Nurumbetov, G., Chen, R., Ballard, N., Bon, S.A.F., 2013. Multicompartmental Janus Microbeads from Branched Polymers by Single-Emulsion Droplet Microfluidics. Langmuir 29, 12657-12662.

Chen, Y.P., Gao, W., Zhang, C.B., Zhao, Y.J., 2016. Three-dimensional splitting microfluidics. Lab Chip 16, 1332-1339.

Chuah, A.M., Kuroiwa, T., Kobayashi, I., Zhang, X., Nakajima, M., 2009. Preparation of uniformly sized alginate microspheres using the novel combined methods of microchannel emulsification and external gelation. Colloids Surf., A 351, 9-17.

Cordero, M.L., Gallaire, F., Baroud, C.N., 2011. Quantitative analysis of the dripping and jetting regimes in co-flowing capillary jets. Phys. Fluids 23, 094111.

Damiati, S., Kompella, U.B., Damiati, S.A., Kodzius, R., 2018. Microfluidic Devices for Drug Delivery Systems and Drug Screening. Genes 9, 103.

Dangla, R., Kayi, S.C., Baroud, C.N., 2013. Droplet microfluidics driven by gradients of confinement. Proc. Natl. Acad. Sci. USA 110, 853-858.

Datta, S.S., Abbaspourrad, A., Amstad, E., Fan, J., Kim, S.H., Romanowsky, M., Shum, H.C., Sun, B.J., Utada, A.S., Windbergs, M., Zhou, S.B., Weitz, D.A., 2014. 25th Anniversary Article: Double Emulsion Templated Solid Microcapsules: Mechanics And Controlled Release. Adv. Mater. 26, 2205-2218.

Ding, A.G., Schwendeman, S.P., 2008. Acidic Microclimate pH Distribution in PLGA Microspheres Monitored by Confocal Laser Scanning Microscopy. Pharm. Res. 25, 2041-2052.

Ding, Y., Solvas, X.C.I., Demello, A., 2015. "V-junction": a novel structure for high-speed generation of bespoke droplet flows. Analyst 140, 414-421.

Dutka, F., Opalski, A.S., Garstecki, P., 2016. Nano-liter droplet libraries from a pipette: step emulsificator that stabilizes droplet volume against variation in flow rate. Lab Chip 16, 2044-2049.

Eberhardt, A., Boskovic, D., Loebbecke, S., Panic, S., Winter, Y., 2019. Customized Design of Scalable Microfluidic Droplet Generators Using Step-Emulsification Methods. Chem. Eng. Technol. 42, 2195-2201.

Eggersdorfer, M.L., Zheng, W., Nawar, S., Mercandetti, C., Ofner, A., Leibacher, I., Koehler, S., Weitz, D.A., 2017. Tandem emulsification for high-throughput production of double emulsions. Lab Chip 17, 936-942.

Eggersdorfer, M.L., Seybold, H., Ofner, A., Weitz, D.A., Studart, A.R., 2018. Wetting controls of droplet formation in step emulsification. Proc. Natl. Acad. Sci. USA 115, 9479-9484.

Ekanem, E.E., Nabavi, S.A., Vladisavljevic, G.T., Gu, S., 2015. Structured Biodegradable Polymeric Microparticles for Drug Delivery Produced Using Flow Focusing Glass Microfluidic Devices. ACS Appl. Mater. Interfaces 7, 23132-23143.

Femmer, T., Jans, A., Eswein, R., Anwar, N., Moeller, M., Wessling, M., Kuehne, A.J.C., 2015. High-Throughput Generation of Emulsions and Microgels in Parallelized Microfluidic Drop-Makers Prepared by Rapid Prototyping. ACS Appl. Mater. Interfaces 7, 12635-12638.

Feng, K., Gao, N., Zhang, M.L., Zhou, K., Dong, H., Wang, P., Tian, L., He, G.K., Li, G.T., 2019. Creation of Nonspherical Microparticles through Osmosis-Driven Arrested Coalescence of Microfluidic Emulsions. Small, 1903884.

Friess, F., Nöchel, U., Lendlein, A., Wischke, C., 2014. Polymer Micronetworks with Shape-Memory as Future Platform to Explore Shape-Dependent Biological Effects. Adv. Healthcare Mater. 3, 1986-1990.

1152 Friess, F., Lendlein, A., Wischke, C., 2016. Two phase microfluidics with inviscid drops: Effects of total flow rate
1153 and delayed surfactant addition. MRS Adv. 1, 2019-2024.

1154 Friess, F., Roch, T., Seifert, B., Lendlein, A., Wischke, C., 2019. Phagocytosis of spherical and ellipsoidal
1155 micronetwork colloids from crosslinked poly(epsilon-caprolactone). Int. J. Pharm. 567, 118461.

1156 Fu, X., Hosta-Rigau, L., Chandrawati, R., Cui, J., 2018. Multi-Stimuli-Responsive Polymer Particles, Films, and
1157 Hydrogels for Drug Delivery. Chem 4, 2084-2107.

1158 Ganneboyina, S.R., Ghatak, A., 2013. Multi-helical micro-channels for rapid generation of drops of water in oil.
1159 Microfluid. Nanofluid. 15, 637-646.

1160 Garstecki, P., Fuerstman, M.J., Stone, H.A., Whitesides, G.M., 2006. Formation of droplets and bubbles in a
1161 microfluidic T-junction - scaling and mechanism of break-up. Lab Chip 6, 437-446.

1162 Gregoritza, M., Abstiens, K., Graf, M., Goepferich, A.M., 2018. Fabrication of antibody-loaded microgels using
1163 microfluidics and thiol-ene photoclick chemistry. Eur. J. Pharm. Biopharm. 127, 194-203.

1164 Hackelbusch, S., Rossow, T., Steinhilber, D., Weitz, D.A., Seiffert, S., 2015. Hybrid Microgels with Thermo-
1165 Tunable Elasticity for Controllable Cell Confinement. Adv. Healthcare Mater. 4, 1841-1848.

1166 Hasturk, O., Kaplan, D.L., 2019. Cell armor for protection against environmental stress: Advances, challenges and
1167 applications in micro- and nanoencapsulation of mammalian cells. Acta Biomater. 95, 3-31.

1168 Hati, A.G., Bassett, D.C., Ribe, J.M., Sikorski, P., Weitz, D.A., Stokke, B.T., 2016. Versatile, cell and chip friendly
1169 method to gel alginate in microfluidic devices. Lab Chip 16, 3718-3727.

1170 Hati, A.G., Szymborski, T.R., Steinacher, M., Amstad, E., 2018. Production of monodisperse drops from viscous
1171 fluids. Lab Chip 18, 648-654.

1172 He, T.X., Liang, Q.L., Zhang, K., Mu, X., Luo, T.T., Wang, Y.M., Luo, G.A., 2011. A modified microfluidic chip
1173 for fabrication of paclitaxel-loaded poly(l-lactic acid) microspheres. Microfluid. Nanofluid. 10, 1289-1298.

1174 Herranz-Blanco, B., Ginestar, E., Zhang, H.B., Hirvonen, J., Santos, H.A., 2017. Microfluidics platform for glass
1175 capillaries and its application in droplet and nanoparticle fabrication. Int. J. Pharm. 516, 100-105.

1176 Holtze, C., 2013. Large-scale droplet production in microfluidic devices-an industrial perspective. J. Phys. D:
1177 Appl. Phys. 46, 114008.

1178 Hou, F.L., Zhu, Y.H., Zou, Q., Zhang, C., Wang, H., Liao, Y.G., Wang, Q., Yang, X.L., Yang, Y.J., 2019. One-
1179 step preparation of multifunctional alginate microspheres loaded with in situ-formed gold nanostars as a
1180 photothermal agent. Mater. Chem. Front. 3, 2018-2024.

1181 Huang, P., Wang, X., Liang, X., Yang, J., Zhang, C., Kong, D., Wang, W., 2019. Nano-, micro-, and macroscale
1182 drug delivery systems for cancer immunotherapy. Acta Biomater. 85, 1-26.

1183 Hung, L.H., Teh, S.Y., Jester, J., Lee, A.P., 2010. PLGA micro/nanosphere synthesis by droplet microfluidic
1184 solvent evaporation and extraction approaches. Lab Chip 10, 1820-1825.

1185 Jafarifar, E., Hajialyani, M., Akbari, M., Rahimi, M., Shokoohinia, Y., Fattahi, A., 2017. Preparation of a
1186 reproducible long-acting formulation of risperidone-loaded PLGA microspheres using microfluidic method.
1187 Pharm. Dev. Technol. 22, 836-843.

1188 Jeong, E.S., Son, H.A., Kim, M.K., Park, K.H., Kay, S., Chae, P.S., Kim, J.W., 2014. Fabrication of monodisperse
1189 liposomes-in-microgel hybrid microparticles in capillary-based microfluidic devices. Colloids Surf., B 123, 339-
1190 344.

1191 Jeong, W.C., Lim, J.M., Choi, J.H., Kim, J.H., Lee, Y.J., Kim, S.H., Lee, G., Kim, J.D., Yi, G.R., Yang, S.M.,
1192 2012. Controlled generation of submicron emulsion droplets via highly stable tip-streaming mode in microfluidic
1193 devices. Lab Chip 12, 1446-1453.

1194 Josephides, D.N., Sajjadi, S., 2015. Increased Drop Formation Frequency via Reduction of Surfactant Interactions
1195 in Flow-Focusing Microfluidic Devices. Langmuir 31, 1218-1224.

1196 Kamperman, T., Trikalitis, V.D., Karperien, M., Visser, C.W., Leijten, J., 2018. Ultrahigh-Throughput Production
1197 of Monodisperse and Multifunctional Janus Microparticles Using in-Air Microfluidics. ACS Appl. Mater.
1198 Interfaces 10, 23433-23438.

1199 Kauscher, U., Holme, M.N., Björnmalm, M., Stevens, M.M., 2019. Physical stimuli-responsive vesicles in drug
1200 delivery: Beyond liposomes and polymersomes. Adv. Drug Delivery Rev. 138, 259-275.

Keohane, K., Brennan, D., Galvin, P., Griffin, B.T., 2014. Silicon microfluidic flow focusing devices for the production of size-controlled PLGA based drug loaded microparticles. Int. J. Pharm. 467, 60-69.

Khalid, N., Kobayashi, I., Uemura, K., Nakajima, M., 2017. Asymmetrical Microchannel Emulsification Plates for Production of Small-Sized Monodispersed Emulsion Droplets. Chem. Eng. Technol. 40, 2351-2355.

Khan, I.U., Serra, C.A., Anton, N., Li, X., Akasov, R., Messaddeq, N., Kraus, I., Vandamme, T.F., 2014. Microfluidic conceived drug loaded Janus particles in side-by-side capillaries device. Int. J. Pharm. 473, 239-249.

Khan, I.U., Serra, C.A., Anton, N., Er-Rafik, M., Blanck, C., Schmutz, M., Kraus, I., Messaddeq, N., Sutter, C., Anton, H., Klymchenko, A.S., Vandamme, T.F., 2015a. Microfluidic conceived Trojan microcarriers for oral delivery of nanoparticles. Int. J. Pharm. 493, 7-15.

Khan, I.U., Stolch, L., Serra, C.A., Anton, N., Akasov, R., Vandamme, T.F., 2015b. Microfluidic conceived pH sensitive core-shell particles for dual drug delivery. Int. J. Pharm. 478, 78-87.

Kim, H.G., Kim, K.M., Kim, Y.H., Lee, S.H., Kim, G.M., 2013a. Preparation of Monodisperse ENX-Loaded PLGA Microspheres Using a Microfluidic Flow-Focusing Device. J. Biobased Mater. Bioenergy 7, 108-114.

Kim, S.H., Kim, J.W., Kim, D.H., Han, S.H., Weitz, D.A., 2013b. Enhanced-throughput production of polymersomes using a parallelized capillary microfluidic device. Microfluid. Nanofluid. 14, 509-514.

Kinoshita, K., Parra, E., Hussein, A., Utoft, A., Walke, P., de Bruijn, R., Needham, D., 2016. From Single Microparticles to Microfluidic Emulsification: Fundamental Properties (Solubility, Density, Phase Separation) from Micropipette Manipulation of Solvent, Drug and Polymer Microspheres. Processes 4, 49.

Klinger, D., Landfester, K., 2012. Stimuli-responsive microgels for the loading and release of functional compounds: Fundamental concepts and applications. Polymer 53, 5209-5231.

Kobayashi, I., Neves, M.A., Wada, Y., Uemura, K., Nakajima, M., 2012. Large microchannel emulsification device for mass producing uniformly sized droplets on a liter per hour scale. Green Process. Synth. 1, 353-362.

Kong, T., Wu, J., Yeung, K.W.K., To, M.K.T., Shum, H.C., Wang, L., 2013. Microfluidic fabrication of polymeric core-shell microspheres for controlled release applications. Biomicrofluidics 7, 044128.

Krüger, A.J.D., Bakirman, O., Guerzoni, L.P.B., Jans, A., Gehlen, D.B., Rommel, D., Haraszti, T., Kuehne, A.J.C., De Laporte, L., 2019. Compartmentalized Jet Polymerization as a High-Resolution Process to Continuously Produce Anisometric Microgel Rods with Adjustable Size and Stiffness. Adv. Mater. 31, 1903668.

Labie, H., Perro, A., Lapeyre, V., Goudeau, B., Catargi, B., Auzély, R., Ravaine, V., 2019. Sealing hyaluronic acid microgels with oppositely-charged polypeptides: A simple strategy for packaging hydrophilic drugs with on-demand release. J. Colloid Interface Sci. 535, 16-27.

Lashkaripour, A., Rodriguez, C., Ortiz, L., Densmore, D., 2019. Performance tuning of microfluidic flow-focusing droplet generators. Lab Chip 19, 1041-1053.

Lee, B.K., Yun, Y., Park, K., 2016. PLA micro- and nano-particles. Adv. Drug Delivery Rev. 107, 176-191.

Lee, T.Y., Ku, M., Kim, B., Lee, S., Yang, J., Kim, S.H., 2017. Microfluidic Production of Biodegradable Microcapsules for Sustained Release of Hydrophilic Actives. Small 13, 1700646.

Lee, S., Lee, T.Y., Amstad, E., Kim, S.H., 2018. Microfluidic Production of Capsules-in-Capsules for Programed Release of Multiple Ingredients. Adv Mater Technol-Us 3, 1800006.

Leon, R.A.L., Somasundar, A., Badruddoza, A.Z.M., Khan, S.A., 2015. Microfluidic Fabrication of Multi-Drug-Loaded Polymeric Microparticles for Topical Glaucoma Therapy. Part. Part. Syst. Charact. 32, 567-572.

Li, W., Pharn, H.H., Nie, Z., MacDonald, B., Guenther, A., Kumacheva, E., 2008a. Multi-step microfluidic polymerization reactions conducted in droplets: The internal trigger approach. J. Am. Chem. Soc. 130, 9935-9941.

Li, W., Young, E.W.K., Seo, M., Nie, Z., Garstecki, P., Simmons, C.A., Kumacheva, E., 2008b. Simultaneous generation of droplets with different dimensions in parallel integrated microfluidic droplet generators. Soft Matter 4, 258-262.

Li, Z., Mak, S.Y., Sauret, A., Shum, H.C., 2014. Syringe-pump-induced fluctuation in all-aqueous microfluidic system implications for flow rate accuracy. Lab Chip 14, 744-749.

Li, Z., Leshansky, A.M., Pismen, L.M., Tabeling, P., 2015. Step-emulsification in a microfluidic device. Lab Chip 15, 1023-1031.

Li, X.Y., Jiang, X.Y., 2018. Microfluidics for producing poly (lactic-co-glycolic acid)-based Check for pharmaceutical nanoparticles. Adv. Drug Delivery Rev. 128, 101-114.

Li, W., Zhang, L.Y., Ge, X.H., Xu, B.Y., Zhang, W.X., Qu, L.L., Choi, C.H., Xu, J.H., Zhang, A., Lee, H.M., Weitz, D.A., 2018. Microfluidic fabrication of microparticles for biomedical applications. Chem. Soc. Rev. 47, 5646-5683.

Li, R., Kobayashi, I., Zhang, Y.R., Neves, M.A., Uemura, K., Nakajima, M., 2019a. Preparation of monodisperse W/O emulsions using a stainless-steel microchannel emulsification chip. Part. Sci. Technol. 37, 68-73.

Li, Z.D., Li, L.Q., Liao, M.X., He, L.Q., Wu, P., 2019b. Multiple splitting of droplets using multi-furcating microfluidic channels. Biomicrofluidics 13, 024112.

Liang, H., Nacharaju, P., Friedman, A., Friedman, J.M., 2015. Nitric oxide generating/releasing materials. Future Sci. OA 1, FSO54.

Lim, J., Caen, O., Vrignon, J., Konrad, M., Taly, V., Baret, J.C., 2015. Parallelized ultra-high throughput microfluidic emulsifier for multiplex kinetic assays. Biomicrofluidics 9, 034101.

Liu, D.F., Zhang, H.B., Fontana, F., Hirvonen, J.T., Santos, H.A., 2017. Microfluidic-assisted fabrication of carriers for controlled drug delivery. Lab Chip 17, 1856-1883.

Liu, D.F., Zhang, H.B., Fontana, F., Hirvonen, J.T., Santos, H.A., 2018. Current developments and applications of microfluidic technology toward clinical translation of nanomedicines. Adv. Drug Delivery Rev. 128, 54-83.

Loizou, K., Wong, V.-L., Hewakandamby, B., 2018. Examining the Effect of Flow Rate Ratio on Droplet Generation and Regime Transition in a Microfluidic T-Junction at Constant Capillary Numbers. Inventions 3, 54.

Lundström, E.A., Rencken, R.K., van Wyk, J.H., Coetzee, L.J.E., Bahlmann, J.C.M., Reif, S., Strasheim, E.A., Bigalke, M.C., Pontin, A.R., Goedhals, L., Steyn, D.G., Heyns, C.F., Aldera, L.A., Mackenzie, T.M., Purcea, D., Grosgurin, P.Y., Porchet, H.C., 2009. Triptorelin 6-Month Formulation in the Management of Patients with Locally Advanced and Metastatic Prostate Cancer. Clin. Drug Invest. 29, 757-765.

Martino, C., Berger, S., Wootton, R.C.R., Demello, A.J., 2014. A 3D-printed microcapillary assembly for facile double emulsion generation. Lab Chip 14, 4178-4182.

Matthew, A.H., Saurabh, K., Ali, B., Paul, S.C., 2003. Microfluidic diffusion diluter: bulging of PDMS microchannels under pressure-driven flow. J. Micromech. Microeng. 13, 412.

Mazutis, L., Vasiliauskas, R., Weitz, D.A., 2015. Microfluidic Production of Alginate Hydrogel Particles for Antibody Encapsulation and Release. Macromol. Biosci. 15, 1641-1646.

Min, Y., Moon, G.D., Kim, C.E., Lee, J.H., Yang, H., Soon, A., Jeong, U., 2014. Solution-based synthesis of anisotropic metal chalcogenide nanocrystals and their applications. J. Mater. Chem. C 2, 6222-6248.

Mittal, N., Cohen, C., Bibette, J., Bremond, N., 2014. Dynamics of step-emulsification: From a single to a collection of emulsion droplet generators. Phys. Fluids 26, 082109.

Moyle, T.M., Walker, L.M., Anna, S.L., 2013. Controlling thread formation during tipstreaming through an active feedback control loop. Lab Chip 13, 4534-4541.

Nabavi, S.A., Vladisavljevic, G.T., Bandulasena, M.V., Arjmandi-Tash, O., Manovic, V., 2017a. Prediction and control of drop formation modes in microfluidic generation of double emulsions by single-step emulsification. J. Colloid Interface Sci. 505, 315-324.

Nabavi, S.A., Vladisavljevic, G.T., Manovic, V., 2017b. Mechanisms and control of single-step microfluidic generation of multi-core double emulsion droplets. Chem. Eng. J. 322, 140-148.

Nakajima, M., 2017. Comment on "Robust scalable high throughput production of monodisperse drops" by E. Amstad, M. Chemama, M. Eggersdorfer, L. R. Arriaga, M. P. Brenner and D. A. Weitz, Lab Chip, 2016, 16, 4163. Lab Chip 17, 2330-2331.

Nisisako, T., Torii, T., 2008. Microfluidic large-scale integration on a chip for mass production of monodisperse droplets and particles. Lab Chip 8, 287-293.

Nisisako, T., Ando, T., Hatsuzawa, T., 2012. High-volume production of single and compound emulsions in a microfluidic parallelization arrangement coupled with coaxial annular world-to-chip interfaces. Lab Chip 12, 3426-3435.

Nys, G., Fillet, M., 2018. Microfluidics contribution to pharmaceutical sciences: From drug discovery to post marketing product management. J. Pharm. Biomed. Anal. 159, 348-362.

Ofner, A., Moore, D.G., Ruhs, P.A., Schwendimann, P., Eggersdorfer, M., Amstad, E., Weitz, D.A., Studart, A.R., 2017. High-Throughput Step Emulsification for the Production of Functional Materials Using a Glass Microfluidic Device. Macromol. Chem. Phys. 218, 1600472.

Ofner, A., Mattich, I., Hagander, M., Dutto, A., Seybold, H., Ruhs, P.A., Studart, A.R., 2019. Controlled Massive Encapsulation via Tandem Step Emulsification in Glass. Adv. Funct. Mater. 29.

Park, K., Skidmore, S., Hadar, J., Garner, J., Park, H., Otte, A., Soh, B.K., Yoon, G., Yu, D., Yun, Y., Lee, B.K., Jiang, X., Wang, Y., 2019. Injectable, long-acting PLGA formulations: Analyzing PLGA and understanding microparticle formation. J. Controlled Release 304, 125-134.

Pessi, J., Santos, H.A., Miroshnyk, I., JoukoYliruusi, Weitz, D.A., Mirza, S., 2014. Microfluidics-assisted engineering of polymeric microcapsules with high encapsulation efficiency for protein drug delivery. Int. J. Pharm. 472, 82-87.

Plamper, F.A., Richtering, W., 2017. Functional Microgels and Microgel Systems. Acc. Chem. Res. 50, 131-140.

Polenz, I., Weitz, D.A., Baret, J.C., 2015. Polyurea Microcapsules in Microfluidics: Surfactant Control of Soft Membranes. Langmuir 31, 1127-1134.

Qi, F., Wu, J., Li, H., Ma, G.H., 2019. Recent research and development of PLGA/PLA microspheres/nanoparticles: A review in scientific and industrial aspects. Front. Chem. Sci. Eng. 13, 14-27.

Ramazani, F., Chen, W.L., van Nostrum, C.F., Storm, G., Kiessling, F., Lammers, T., Hennink, W.E., Kok, R.J., 2016. Strategies for encapsulation of small hydrophilic and amphiphilic drugs in PLGA microspheres: State-of-the-art and challenges. Int. J. Pharm. 499, 358-367.

Romanowsky, M.B., Abate, A.R., Rotem, A., Holtze, C., Weitz, D.A., 2012. High throughput production of single core double emulsions in a parallelized microfluidic device. Lab Chip 12, 802-807.

Romero, P.A., Abate, A.R., 2012. Flow focusing geometry generates droplets through a plug and squeeze mechanism. Lab Chip 12, 5130-5132.

Sakai, S., Nakahata, M., 2017. Horseradish Peroxidase Catalyzed Hydrogelation for Biomedical, Biopharmaceutical, and Biofabrication Applications. Chem. - Asian J. 12, 3098-3109.

Seiffert, S., Friess, F., Lendlein, A., Wischke, C., 2015. Faster droplet production by delayed surfactant-addition in two-phase microfluidics to form thermo-sensitive microgels. J. Colloid Interface Sci. 452, 38-42.

Shah, J.C., Maniar, M., 1993. pH-Dependent solubility and dissolution of bupivacaine and its relevance to the formulation of a controlled release system. J. Controlled Release 23, 261-270.

Shah, R.K., Shum, H.C., Rowat, A.C., Lee, D., Agresti, J.J., Utada, A.S., Chu, L.Y., Kim, J.W., Fernandez-Nieves, A., Martinez, C.J., Weitz, D.A., 2008. Designer emulsions using microfluidics. Mater. Today 11, 18-27.

Shao, T., Feng, X.L., Jin, Y., Cheng, Y., 2013. Controlled production of double emulsions in dual-coaxial capillaries device for millimeter-scale hollow polymer spheres. Chem. Eng. Sci. 104, 55-63.

Steinacher, M., Du, H., Gilbert, D., Amstad, E., 2019. Production of Additive-Free Amorphous Nanoparticles with a SAW-Based Microfluidic Spray-Dryer. Adv Mater Technol-Us 4, 1800665.

Stolovicki, E., Ziblat, R., Weitz, D.A., 2018. Throughput enhancement of parallel step emulsifier devices by shear-free and efficient nozzle clearance. Lab Chip 18, 132-138.

Studart, A.R., Shum, H.C., Weitz, D.A., 2009. Arrested Coalescence of Particle-coated Droplets into Nonspherical Supracolloidal Structures. J. Phys. Chem. B 113, 3914-3919.

Takechi, N., Ohtani, S., Nagai, A., 2002. Production of Microspheres, EP 0 779 072 B1.

Tan, H., Guo, S., Dinh, N.-D., Luo, R., Jin, L., Chen, C.-H., 2017. Heterogeneous multi-compartmental hydrogel particles as synthetic cells for incompatible tandem reactions. Nat. Commun. 8, 663.

Tang, S.K.Y., Whitesides, G.M., 2010. Basic Microfluidic and Soft Lithographic Techniques, in: Yeshaiahu, F., Demetri, P., Changhuei, Y. (Eds.), Optofluidics: Fundamentals, Devices, and Applications. McGraw Hill Professional, Access Engineering.

Tetradis-Meris, G., Rossetti, D., de Torres, C.P., Cao, R., Lian, G.P., Janes, R., 2009. Novel Parallel Integration of Microfluidic Device Network for Emulsion Formation. Ind. Eng. Chem. Res. 48, 8881-8889.

Thiele, J., Seiffert, S., 2011. Double emulsions with controlled morphology by microgel scaffolding. Lab Chip 11, 3188-3192.

Tran, T.M., Cater, S., Abate, A.R., 2014. Coaxial flow focusing in poly(dimethylsiloxane) microfluidic devices. Biomicrofluidics 8, 016502.

Tuncaboylu, D.C., Wischke, C., Stormann, F., Lendlein, A., 2017. Microgels from microfluidic templating and photoinduced crosslinking of cinnamylidene acetic acid modified precursors. React. Funct. Polym. 112, 68-73.

Tunn, U.W., Wiedey, K., 2009. Safety and clinical efficacy of a new 6-month depot formulation of leuprorelin acetate in patients with prostate cancer in Europe. Prostate Cancer Prostatic Dis. 12, 83-87.

Utada, A.S., Fernandez-Nieves, A., Stone, H.A., Weitz, D.A., 2007. Dripping to jetting transitions in coflowing liquid streams. Phys. Rev. Lett. 99, 094502.

Vasiliauskas, R., Liu, D.F., Cito, S., Zhang, H.B., Shahbazi, M.A., Sikanen, T., Mazutis, L., Santos, H.A., 2015. Simple Microfluidic Approach to Fabricate Monodisperse Hollow Microparticles for Multidrug Delivery. ACS Appl. Mater. Interfaces 7, 14822-14832.

Visser, C.W., Kamperman, T., Karbaat, L.P., Lohse, D., Karperien, M., 2018. In-air microfluidics enables rapid fabrication of emulsions, suspensions, and 3D modular (bio)materials. Sci. Adv. 4, eaao1175.

Vladisavljevic, G.T., Kobayashi, I., Nakajima, M., 2011. Effect of dispersed phase viscosity on maximum droplet generation frequency in microchannel emulsification using asymmetric straight-through channels. Microfluid. Nanofluid. 10, 1199-1209.

Vladisavljevic, G.T., Shahmohamadi, H., Das, D.B., Ekanem, E.E., Tauanov, Z., Sharma, L., 2014. Glass capillary microfluidics for production of monodispersed poly (DL-lactic acid) and polycaprolactone microparticles: Experiments and numerical simulations. J. Colloid Interface Sci. 418, 163-170.

Vladisavljevic, G.T., Ekanem, E.E., Zhang, Z.L., Khalid, N., Kobayashi, I., Nakajima, M., 2018. Long-term stability of droplet production by microchannel (step) emulsification in microfluidic silicon chips with large number of terraced microchannels. Chem. Eng. J. 333, 380-391.

Wang, J.T., Wang, J., Han, J.J., 2011. Fabrication of Advanced Particles and Particle-Based Materials Assisted by Droplet-Based Microfluidics. Small 7, 1728-1754.

Wang, Y.H., Tumarkin, E., Velasco, D., Abolhasani, M., Lau, W., Kumacheva, E., 2013. Exploring a direct injection method for microfluidic generation of polymer microgels. Lab Chip 13, 2547-2553.

Wischke, C., Schwendeman, S.P., 2008. Principles of encapsulating hydrophobic drugs in PLA/PLGA microparticles. Int. J. Pharm. 364, 298-327.

Wischke, C., Zhang, Y., Mittal, S., Schwendeman, S.P., 2010. Development of PLGA-Based Injectable Delivery Systems For Hydrophobic Fenretinide. Pharm. Res. 27, 2063-2074.

Wischke, C., Schneider, C., Neffe, A.T., Lendlein, A., 2013. Polyalkylcyanoacrylates as in situ formed diffusion barriers in multimaterial drug carriers. J. Controlled Release 169, 321-328.

Wu, J., Kong, T., Yeung, K.W.K., Shum, H.C., Cheung, K.M.C., Wang, L., To, M.K.T., 2013. Fabrication and characterization of monodisperse PLGA–alginate core–shell microspheres with monodisperse size and homogeneous shells for controlled drug release. Acta Biomater. 9, 7410-7419.

Wu, Y., Qian, X., Zhang, M., Dong, Y., Sun, S.Q., Wang, X.H., 2018. Mode Transition of Droplet Formation in a Semi-3D Flow-Focusing Microfluidic Droplet System. Micromachines 9, 139.

Xu, Q.B., Hashimoto, M., Dang, T.T., Hoare, T., Kohane, D.S., Whitesides, G.M., Langer, R., Anderson, D.G., 2009. Preparation of Monodisperse Biodegradable Polymer Microparticles Using a Microfluidic Flow-Focusing Device for Controlled Drug Delivery. Small 5, 1575-1581.

Xu, J., Zhang, S.S., Machado, A., Lecommandoux, S., Sandre, O., Gu, F., Colin, A., 2017a. Controllable Microfluidic Production of Drug-Loaded PLGA Nanoparticles Using Partially Water-Miscible Mixed Solvent Microdroplets as a Precursor. Sci. Rep. 7, 4794.

Xu, X.N., Song, R.Y., He, M.H., Peng, C., Yu, M., Hou, Y.M., Qiu, H.H., Zou, R.H., Yao, S.H., 2017b. Microfluidic production of nanoscale perfluorocarbon droplets as liquid contrast agents for ultrasound imaging. Lab Chip 17, 3504-3513.

Yadavali, S., Jeong, H.H., Lee, D., Issadore, D., 2018. Silicon and glass very large scale microfluidic droplet integration for terascale generation of polymer microparticles. Nat. Commun. 9, 1222.

Yadavali, S., Lee, D.E.Y.O., Issadore, D., 2019. Robust Microfabrication of Highly Parallelized Three-Dimensional Microfluidics on Silicon. Sci. Rep. 9, 12213.

Yu, L., Sun, Q., Hui, Y., Seth, A., Petrovsky, N., Zhao, C.-X., 2019. Microfluidic formation of core-shell alginate microparticles for protein encapsulation and controlled release. J. Colloid Interface Sci. 539, 497-503.

Zhang, H.W., Betz, A., Qadeer, A., Attinger, D., Chen, W.L., 2011. Microfluidic Formation of Monodispersed Spherical Microgels Composed of Triple-Network Crosslinking. J. Appl. Polym. Sci. 121, 3093-3100.

Zhang, Y.R., Kobayashi, I., Wada, Y., Neves, M.A., Uemura, K., Nakajima, M., 2019. Asymmetric straight-through microchannel arrays made of aluminum for producing monodisperse O/W emulsions. Part. Sci. Technol. in press, doi: 10.1080/02726351.2019.1612488

Zhu, P.A., Wang, L.Q., 2017. Passive and active droplet generation with microfluidics: a review. Lab Chip 17, 34-75.